

ISTANBUL TECHNICAL UNIVERSITY ★ INSTITUTE OF ENERGY

CFD MODELLING OF A CLOSE-COUPLED CATALYTIC CONVERTOR

**M.Sc. Thesis by
Esra GEMİCİ**

Department : Energy Science and Technology

Programme : Energy Science and Technology

JUNE 2009

ISTANBUL TECHNICAL UNIVERSITY ★ INSTITUTE OF ENERGY

CFD MODELLING OF A CLOSE-COUPLED CATALYTIC CONVERTOR

**M.Sc. Thesis by
Esra GEMİCİ
(301061010)**

**Date of submission : 05 May 2009
Date of defence examination: 03 June 2009**

**Supervisor (Chairman) : Prof. Dr. Murat AYDIN (ITU)
Members of the Examining Committee : Prof. Dr. Melih GEÇKİNLİ (ITU)
Assis. Prof. Dr. Murat ÇAKAN (ITU)**

JUNE 2009

İSTANBUL TEKNİK ÜNİVERSİTESİ ★ ENERJİ ENSTİTÜSÜ

**CLOSE-COUPLED KATALİTİK KONVERTÖRDE 3 BOYUTLU AKIŞ
ANALİZİ**

**YÜKSEK LİSANS TEZİ
Esra GEMİCİ
(301061010)**

Tezin Enstitüye Verildiği Tarih : 05 Mayıs 2009

Tezin Savunulduğu Tarih : 03 Haziran 2009

**Tez Danışmanı : Prof. Dr. Murat AYDIN (İTÜ)
Diğer Jüri Üyeleri : Prof. Dr. Melih GEÇKİNLİ (İTÜ)
Yrd. Doç. Dr. Murat ÇAKAN (İTÜ)**

HAZİRAN 2009

FOREWORD

I would like to express my sincere appreciation for the assistance given by many people throughout my graduate study. This project would not have been completed on schedule without their help. I first want to express thanks to Prof. Dr. Murat Aydın. As the director of studies, his frequent discussions, and some sparkling ideas have given me great assistance throughout this project. I also wish to thank to my colleagues Cevriye Ünal, İsmail Savcı and Ufuk Yavuz for their enlightening discussions on CFD techniques. Their support on the STAR-CD program is highly appreciated. Thanks are also addressed to my cousins Erdem Akça and Didem Yılmaz for providing a perfect computer support. Finally a special word of thanks goes to my family for their encouragement and support.

June 2009

Esra Gemici

TABLE OF CONTENTS

	<u>Page</u>
ABBREVIATIONS	ix
LIST OF TABLES	xi
LIST OF FIGURES	xiii
SUMMARY	xv
ÖZET	xvii
1. INTRODUCTION	1
2. THEORY AND BACKGROUND	3
2.1 Emission Legislation	3
2.2 Exhaust Gas Composition	4
2.3 Definition of Catalytic Converter	5
2.3.1 Inlet and outlet cones	5
2.3.2 Coated substrate	6
2.3.3 Support material.....	7
2.3.4 Seals	8
2.4 Converter Can (Shell)	10
2.5 Classification of the Catalytic Convertors from Location Point of View	11
2.5.1 Close-coupled catalytic converter	11
2.5.2. Underfloor catalytic converter	12
2.6 Classification of the Catalytic Convertors from Application Point of View	13
2.6.1 Two-way catalytic converter	13
2.6.2. Three-way catalytic converter	15
2.7 Mathematical Modelling of Substrate	18
2.7.1 Catalyst cell shape analysis	21
2.8 Definition of Fundamenal Parameters for Flow Uniformity Prediction	22
2.8.1 Uniformity index (gamma value).....	23
2.8.2 Velocity index	23
2.8.3 Velocity ratio.....	24
2.8.4 High speed area	24
2.8.5 Low speed area.....	24
2.8.6 Pressure Drop	24
2.8.7 Porous Medium	24
2.8.8 Annular Velocity	26
2.9 Theoretical Models.....	27
2.9.2 Conservation of mass	28
2.9.3 Balance of momentum	29
2.9.4 Differencing Schemes	29
2.9.5 Turbulence models	30
3. PROBLEM DEFINITION	33
3.1 Geometrical Constraints	33
3.2 Pyhsical Properties of Substrate	34
3.3 Acceptance Flow Uniformity Criteriaions of the CCC.....	35

4. 3D CFD SIMULATIONS AND RESULTS	37
4.1 Model Set-up and Mesh Structure Application of the Work.....	37
4.2 Boundary Conditions and Constraints.....	38
4.2.1 Porous Medium.....	38
4.3 Post Processing.....	41
4.3.1 First Runner Simulation Results	41
4.3.2 Second Runner Simulation Results	43
4.3.3 Third Runner Simulation Results	45
4.3.4 Fourth Runner Simulation Results	47
4.4 Engine Dynamometer Test.....	49
5. DISCUSSION AND CONCLUSION	51
REFERENCES	53
CURRICULUM VITAE	55

ABBREVIATIONS

A/F	: Air Fuel Ratio
CCC	: Close-Coupled Catalyst
CFD	: Computational Fluid Dynamics
CMS	: Catalyst Monitor Sensor
CPSI	: Cells per Square Inch
CO	: Carbon Monoxide
CO₂	: Carbon Dioxide
DOC	: Diesel Oxidation Catalyst
Fe	: Iron
FV	: Finite Volume
GBD	: Gap Bulk Density
HC	: Hydrocarbons
HEGO	: Heated Exhaust Gas Oxygen
H₂O	: Water
HSD	: High Speed Dynamometer
Ni	: Nickel
NO_x	: Oxides of nitrogen
N₂	: Nitrogen
NSCR	: Non-selective catalytic reduction
OFA	: Open Frontal Area
Pd	: Palladium
PM	: Particulate Matter
Pt	: Platinum
Rh	: Rhodium
SiO₂	: Unisilicate
SO_x	: Oxides of sulphur
SOF	: Soluble Organic Fraction
SULEV	: Super Ultra Low Emission Vehicle
T1	: Tier 1
TiO₂	: Titanium Dioxide
TLEV	: Transitional Low Emission Vehicle
TWC	: Three-way Catalytic Convertors
ULEV	: Ultra Low Emission Vehicle
VI	: Velocity Index
ZEV	: Zero Emission Vehicles

LIST OF TABLES

	<u>Page</u>
Table 3.1: Physical Properties of Substrate	34
Table 3.2: CFD Acceptance Criteria of the Catalytic Convertor.	35
Table 3.3: Target Values for Catalytic Convertor CFD	36
Table 4.1: Boundary Conditions	39
Table 4.2: Result Table of CFD Analysis of First Runner	43
Table 4.3: Result Table of CFD Analysis of Second Runner	45
Table 4.4: Result Table of CFD Analysis of Third Runner	47
Table 4.5: Result Table of CFD Analysis of Fourth Runner	49

LIST OF FIGURES

	<u>Page</u>
Figure 2.1 : Normalized representative tailpipe standards for US, Europe two line and Japan	3
Figure 2.2 : Emission standards for hydrocarbons and nitrogen oxides	4
Figure 2.3 : Catalytic Convertor.	5
Figure 2.4 : Different Types of Catalytic Convertor	6
Figure 2.5 : Ceramic Substrate.....	7
Figure 2.6 : Metallic Substrate	7
Figure 2.7 : Loss of Support Material.	8
Figure 2.8 : Radial Seal.....	9
Figure 2.9 : V-seal.....	10
Figure 2.1 : Axial Seal.	10
Figure 2.11 : Fiat 500 1.2 Lounge Close Coupled Catalyst	12
Figure 2.12 : 2.0 TDCI Titanium Underfloor Catalytic Convertor.....	13
Figure 2.13 : Detailed Section Of Alumina Washcoat.....	14
Figure 2.14 : A/F Ratio VS. Species Conversion Efficiency.....	16
Figure 2.15 : Exhaust System with Underbody Catalytic Convertor.....	17
Figure 2.16 : Cumulative HC emission from cold start for vehicle with UNC.	18
Figure 2.17 : Residual Pressure Drop according vs channel velocity.....	20
Figure 2.18 : Model and Experiment for Uncoated Substrates.....	21
Figure 2.19 : Shapes of square cell, equilateral triangular cell and hexagonal cell .	21
Figure 2.20 : Velocity Index	24
Figure 2.21 : Annular Velocity Plot of an Oval Substrate.	27
Figure 2.22 : CFD Process Overview.	28
Figure 2.23 : Conservation of Mass	29
Figure 3.1 : Geometry Details of the CCC.....	34
Figure 3.2 : Catalyst Gas Flow Distribution Plot of the CCC	36
Figure 4.1 : CFD mesh model used in the simulations	37
Figure 4.2 : Simulation boundary set up plot for permability and porosity factor	40
Figure 4.3 : CCC Geometry Details	41
Figure 4.4 : FLUENT Catalyst Gas Flow Distribution Plot of First Runner	41
Figure 4.5 : STAR-CD Catalyst Gas Flow Distribution Plot of First Runner	42
Figure 4.6 : FLUENT Catalyst Gas Flow Distribution Plot of Second Runner....	43
Figure 4.7 : STAR-CD Catalyst Gas Flow Distribution Plot of Second Runner...	44
Figure 4.8 : FLUENT Catalyst Gas Flow Distribution Plot of Third Runner	45
Figure 4.9 : STAR-CD Catalyst Gas Flow Distribution Plot of Third Runner.....	46
Figure 4.10 : FLUENT Catalyst Gas Flow Distribution Plot of Fourth Runner.....	47
Figure 4.11 : STAR-CD Catalyst Gas Flow Distribution Plot of Fourth Runner....	48
Figure 4.12 : CCC Instalation During HSD Test	50
Figure 4.13 : CCC Brick Inlet and Outlet After HSD test	50

CFD MODELLING OF A CLOSE-COUPLED CATALYTIC CONVERTOR

SUMMARY

Emission legislation standard is one of the most important concepts of the recent years which is becoming more stringent day by day. A uniform flow distribution at converter inlet is one of the fundamental requirements to reduce motor vehicle emissions as the non-uniform flow in the catalytic converter affects catalyst warm-up, light-off time, conversion efficiency, pressure drop, and overall aftertreatment system.

Over last decade most efforts have been directed to catalytic converter CFD analyses as results are reasonable and experimental methods are time and money consuming. Improved catalyst technology helps to decrease light-off temperatures, increase conversion efficiency and make aging characteristics of the catalyst better. Close coupled catalysts are used in most of the vehicles today in order to take the advantage of being close to engine resulting in higher temperature values which is important for the light off time. However, close coupled catalyst's flow uniformity performance is worse than the underbody catalytic converters due to pulsating flow.

In this study, 3D CFD simulations were performed in order to determine the gas flow distribution through the catalyst brick. 3-D CFD simulations were performed using STAR-CD Version 3.26 and FLUENT 6.3 solver to compare the results' accuracy. Identifying geometry, generating the grid, setting up the model, computing and monitoring the solution process, postprocessing the results are the basic steps of this study. Through co-simulation velocity profiles of STAR-CD code and FLUENT code are correlated fairly well

CLOSE-COUPLED KATALİTİK KONVERTÖRDE 3 BOYUTLU AKIŞ ANALİZİ

ÖZET

Gün geçtikçe sıkılaştırılan egzoz emisyon standartları ile ilgili kanunlar son yılların en önemli kavramlarından biri haline gelmiştir. Katalitik konvektördeki akış profilinin dönüştürücünün kimyasal aktivasyonu sağlayacak ısıya ve zamana ulaşması, kimyasal reaksiyonun verimi, basınç kaybı ve bütün egzoz emisyon sistemi üzerinde oldukça büyük bir etkisi vardır. Bu yüzden katalitik konvertörlerin girişindeki akış profilinin düzgün ve eşit dağılması taşıt emisyon değerleri açısından en temel gerekliliği oluşturmaktadır.

Katalitik konvektörlerdeki 3 boyutlu akış analizi, sonuçların kabul edilebilir , zaman ve maliyet açısından deneysel yöntemlere göre daha avantajlı olması nedeni ile birçok araştırmaya konu olmuştur. Gelişen katalist teknolojisi ile kimyasal aktivasyon sıcaklığı düşürülmekte, reaksiyon verimi yükseltilmekte ve daha başarılı yaşlanma profili yakalanmaktadır. Motora daha yakın olmanın kimyasal aktivasyon zamanı açısından daha yüksek giriş sıcaklığı avantajını kullanan close coupled katalistler bugün birçok taşıt teknolojisinde kullanılmaktadır. Bununla birlikte close coupled katalistlerin akış profilindeki dağılım, motordan gelen titreşimli egzoz gazı akışına olan yakınlığından dolayı taşıt gövdesi altına yerleştirilen katalistlerin dağılımına göre daha kötü durumdadır.

Bu çalışmada katalitik konvektörlerdeki akış dağılımı 3 boyutlu olarak incelenmiştir. 3 boyutlu akış analizleri STAR-CD program kodunun 3.26 ve FLUENT program kodunun 6.3 versiyonları kullanılmış sonuç değerleri karşılaştırılmıştır. Geometrinin belirlenmesi, sonlu elemanlar modelinin oluşturulması, kısıtların ve çözüm metotlarının belirlenmesi, programın çalıştırılması ve sonuçların görüntülenmesi bu çalışmanın temel adımlarıdır. Çalışma sonucunda her iki kod ile elde edilen akış dağılım değerleri birbirleri ile tatmin edici bir şekilde uyum göstermiştir

1. INTRODUCTION

As the emissions legislations become more stringent year after year, the research on design parameters affecting the catalytic converters efficiency are accelerated. Warm-up, conversion, overall utilisation efficiency, pressure drop, life and light-off time of catalytic convertors are considered to be the design parameters. Optimization of vehicle, aftertreatment, engine, and fuel concepts is required in order to achieve these very low emission levels. Catalytic converter which reduce the harmful gases is necessary in order to meet the current and future stringent emission regulations. Therefore, there is a common sense that effective catalytic converter system design is one of the significant factors for controlling emission.

Internal flow characteristics of the catalytic convertors have been used as a research subject by many researchers from the middle of 1970s. The ongoing efforts of many researches are directed to catalytic convertor conversion efficiency. This efficiency, depending on the mass transfer rate between the catalyst and the exhaust gas passing through the brick, is mainly influenced by flow performance. Maldistributed flow in the catalytic converter increases light off time, pressure drop and decreases conversion efficiency. With the help of growing computational power three-dimensional computer simulation of fluid flow in catalytic convertor has become an efficient engineering application tool which takes the advantage of time and cost compared to experimental studies.

In this study, numerical modelling and simulations were performed to characterise the flow field within catalytic converter systems and to calculate performance index of fluid flow considering uniformity and velocity index as the key parameters. Two different commercial program codes are used in this study in order to correlate the results. Basics of catalytic convertor CFD, emission standarts, catalytic convertor types and definition including the structure, are given thoroughly in second section. Problem definition and target values of the catalytic convertor CFD analysis are covered in third section. Fourth section includes STAR-CD and Fluent model set-ups, then both analysis results compared to the recommended values set by the major

manufacturers. Fourth section also includes high speed dynamometer test as an evidence of analysis. Last section is the section where all the design and simulations are discussed.

2. THEORY AND BACKGROUND

2.1 Emission Legislation

Exhaust emissions limits pursued by government legislation have become more stringent with the rapid upturn on the worldwide automobile usage. First legislation was introduced in California, USA in 1996 [1]. Tail pipe standards of Gasoline vehicle from varied countries for HC and NO_x are shown on the Figure 2.1.

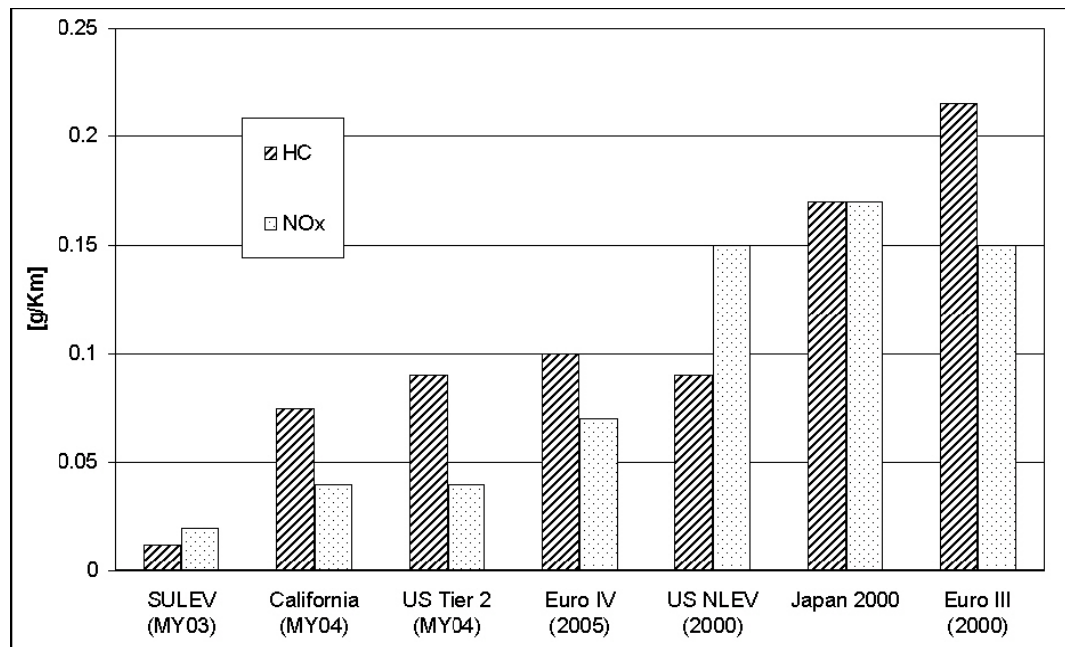


Figure 2.1 : Normalized representative tailpipe standards for US, Europe and Japan.

Emission Standard levels from least clean to cleanest can be listed as T1, TLEV, LEV, ULEV, SULEV, and ZEV. T1 refers to Tier 1 which is the least stringent emission standards; TLEV refers to transitional low emission vehicle which is more stringent than Tier 1 for hydrocarbons (HC). Ultra low emission vehicle (ULEV) takes place between the TLEV and SULEV which is the super ultra low emission vehicle standard even more stringent standard for both HC and NO_x. The strictest emission standard permitting no emissions is zero emission vehicles (ZEV). The emission standards for hydrocarbons and nitrogen oxides graphically are shown on the Figure 2.2 below.

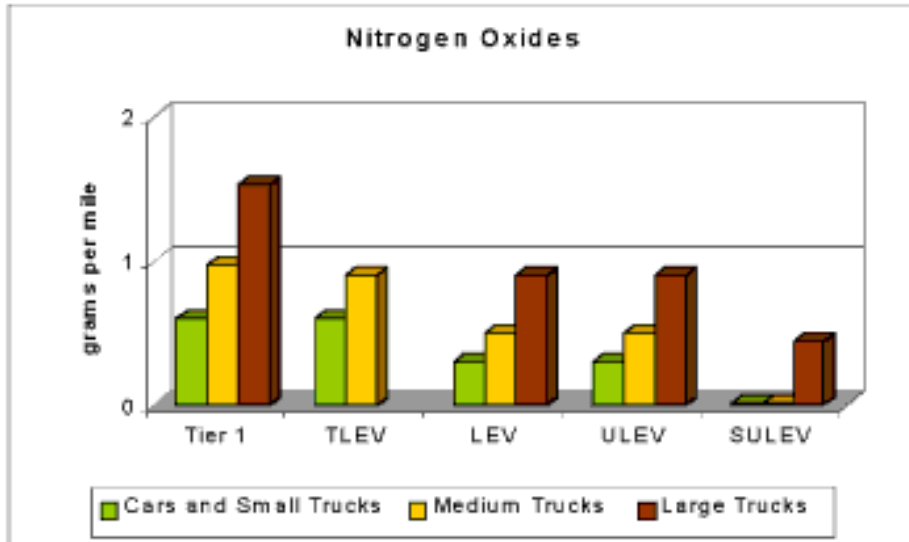


Figure 2.2 : Emission standards for hydrocarbons and nitrogen oxides.

2.2 Exhaust Gas Composition

The basic ingredients of the exhaust gasses that may create harmful atmospheres are carbon monoxide (CO), oxides of nitrogen (NO_x), carbon dioxide (CO₂), oxides of sulphur (SO_x), and particulates. The exhaust also contains water vapour and nitrogen.

The summary of these exhaust gas products is expressed as:

- CO originates from the carbon in unburnt fuel during combustion. Carbon monoxide emissions reduce with increasing excess air. It is colourless as well as odourless and causes asphyxiation by impairing the blood's oxygen absorption.
- CO₂ is not poisonous but it is the fundamental reason of global warming which is known as Green House phenomenon.
- SO_x is formed from the oxidated sulphur in the fuel and lubrication oil during combustion. It poisons the catalysts in the exhaust system and causes acid rains.

NO_x is formed at the high combustion temperatures presented in engine systems. NO is colourless and odourless, NO₂ is reddish-brown gas with a pungent odor. NO_x can irritate the mucous membranes in the respiratory system. It also causes the photochemical smog. Particulates are very little particles of solid carbon soot which

are more likely occur in diesel engines. Absorption of these particules is possible during breathing. They cause health problems as they may be retained in the lungs

2.3 Definition of Catalytic Convertor

Catalytic convertor is a device that reduces the harmful emissions of vehicle exhaust gas. The primary job of the catalytic convertor is to convert the hydrocarbons, carbon monoxide, nitrogen oxides to less harmful gases such as nitrogen, carbon dioxide and water. As seen from the Figure 2.3 below, inlet cone, outlet cone, coated substrate, support material, converter shell, and seals are the main components of catalytic convertor systems.

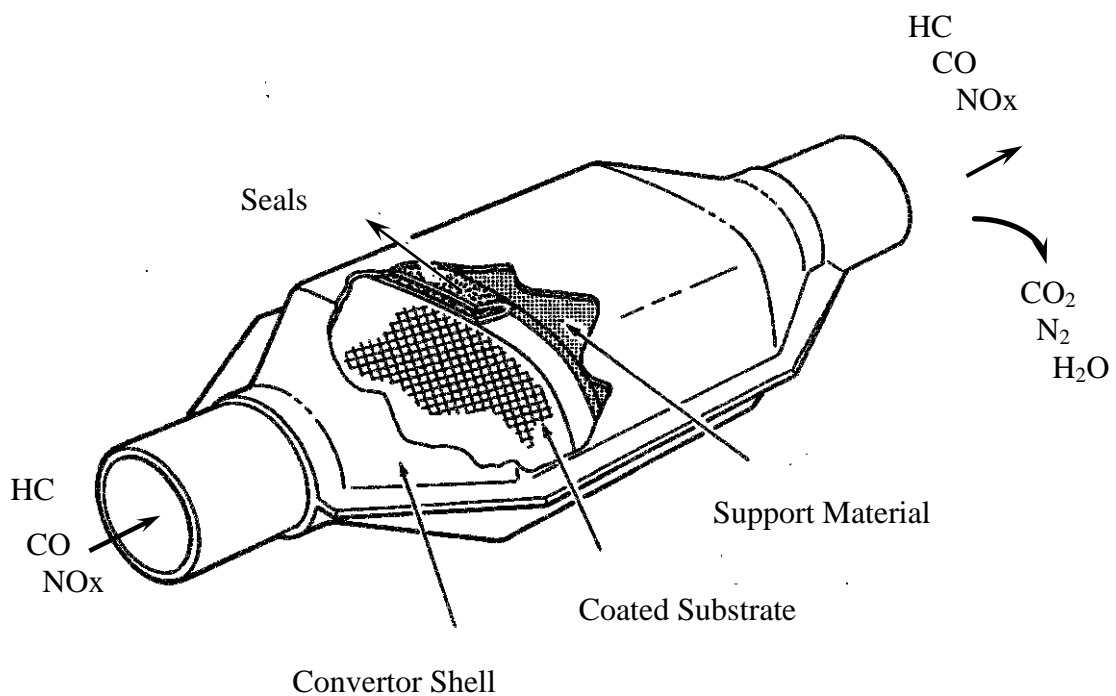


Figure 2.3 : Catalytic Convertor System.

2.3.1 Inlet and Outlet Cones

Inlet and outlet cones have significant impact on catalytic converters performance as the geometry provides flow transition that influences catalyst flow, thermal distribution, catalyst efficiencies, and back pressure. Inlet cone mainly affects the way exhaust gas passes through the catalytic converter therefore flow distribution of coated substrate. Non uniform flow distribution causes local peak velocities and hot spot in the monolith resulting in aging of the catalytic convertor [2]. A uniform distribution over the substrate has a crucial effect on the emission conversion

efficiency as exhaust gas disbands equal to substrate surface area where chemical reaction placed in. Non uniform or bias flow caused by pipe/cone layout results in poor conversion and durability due to heat loss and thermal inertia. Different types of catalytic convertor cone designs are shown on the Figure 2.4 below.

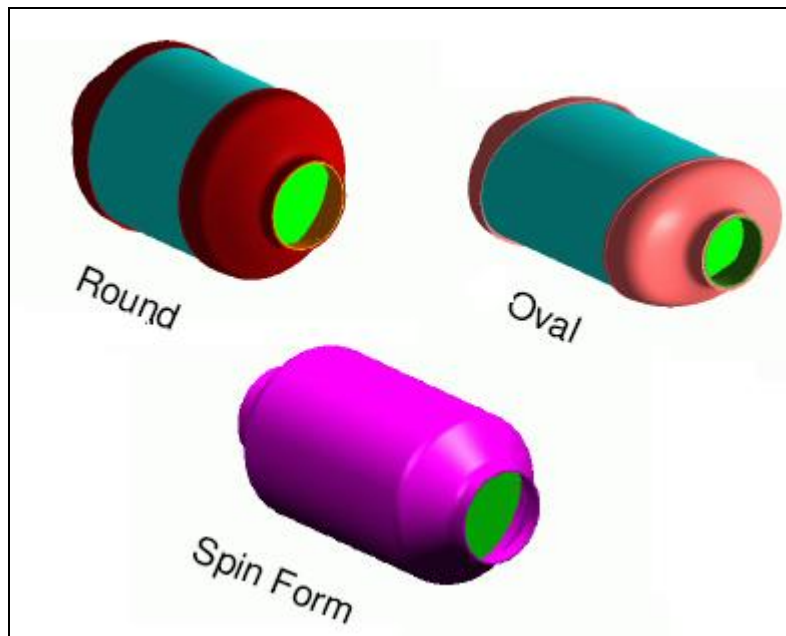


Figure 2.4 : Different types of catalytic convertor.

2.3.2 Coated Substrate

Main purpose of the substrate is to provide a large geometric surface area for catalytic wash coat and active precious metal sites. The key factors of substrate design are minimizing pressure drop and providing higher surface area where the chemical reaction takes place. The chemical reactions are necessary to convert the harmful exhaust gasses to the more environmental ones. Substrates are classified according to their materials as metallic and ceramic. Ceramic substrates need a support system as it is seen on the Figure 2.5 to remain the location stable because of the thermal expansion based on the huge temperature change. Metallic substrates don't require any support as it is directly fixed to its housing (shell) that is shown on Figure 2.6. Ceramic substrates have the advantages of larger geometric surface area, better standard in manufacturing progress, lower thermal expansion, and lighter weight [3]. Although metallic substrates thermal and mechanical shock resistance are better and pressure drop is lower, they are more sensitive to changes in temperature and vibration leading the loss of adherence between wash coat and the substrate structure [4]. Loading of the wash coat is the most effective factor for chemical

reactions. Rhodium, platinum and palladium are the precious metals that have crucial effect on the chemical reaction efficiency. Increased usage of the precious metals means increased effectiveness of process, without changing the substrate surface area but also means more cost.

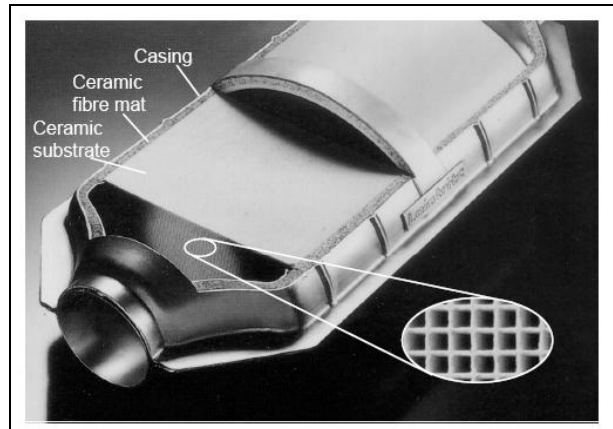


Figure 2.5 : Ceramic Substrate.

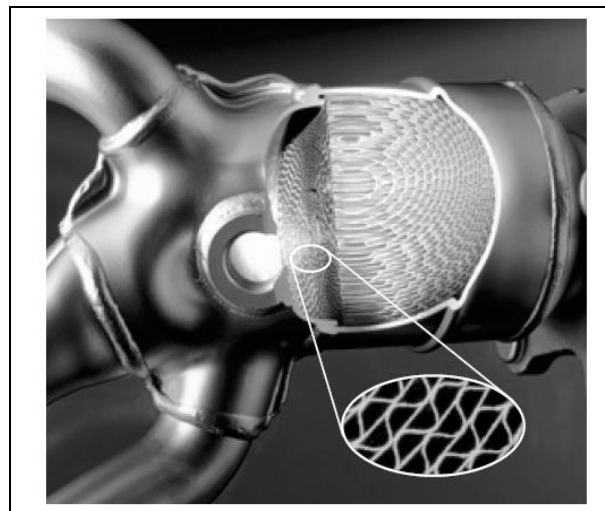


Figure 2.6 : Metallic Substrate.

2.3.3 Support Material

Main purpose of the support material is to provide holding force between the substrate and shell as the catalytic convertor working conditions differ due to the exhaust gas pulsations and temperature difference. Support material plays an important role on controlling the gap expansion between the coated substrate and shell. Mounting pressure changes due to material property. Catalytic convertor support material has a crucial effect on long-term converter efficiency, lifetime and durability. Gap bulk density (GBD) is an important design criterion that any loss on the GBD results in insufficient mat pressure leading mat erosion. The loss in GBD

occurs with the expansion of the shell caused by the temperature inside the convertor exceeding the design temperature limits of the mat. Loss of support material due to edge erosion from pulsating flow can cause flow blockage [5]. As it is seen in the Figure 2.7 below the loss of support material as a result of exceeding material temperature capabilities make the catalytic convertor not functioning. Support material is generally made of either wire mesh or intumescent mat. There are three different types of mat mounts expandable, hybrid and non-expandable. Expandable support materials use the thermal energy to maintain the holding force; they are generally used in gasoline engines as their operation temperature is higher. Hybrid one have both expandable and non-expandable layers. The application area of the non expandable support materials is diesel engines as the support material functional characteristics are not related with the thermal energy and diesel engines operating temperature relatively lower to the gasoline engine.



Figure 2.7 : Loss of Support Material.

2.3.4 Seals

Seals are used to prevent the gas by pass and protect the mat from erosion by blocking the exhaust gas. The seals are generally made of Stainless Steel UNS S31000 (SS310), UNS S66286 (A286) and the combination of these two materials. Axial and/or radial compression characteristics are the main selection criteria's for the seal material. The seals are generally characterized as radial, axial, V and L seal [5]. Radial seal provides the holding force in radial direction. Radial seal also prevents the convertor from leak and erosion. Z seals are one type of radial seals.

Close coupled catalyst and convertors mounted to manifold are the main application areas of Z seals as the temperature of the catalyst inlet is up to 1050 C. In order to meet iso-static strength of the ceramic substrate, the statistical compression range of z-seal, seal density and material characteristic can be changed [5]. Figure 2.8 below shows a representative radial seal.



Figure 2.8 : Radial Seal.

V-seal is used to prevent the exhaust gas from going through the support material with stainless steel knitted wire mesh support. V- seals are used in underbody catalytic convertors where the temperature of the environment is not very high compared to close coupled catalyst location. The efficiency of the exhaust gas passage to support material prevention differs from 95% to 99%. Figure 2.9 below shows a representative V-seal.

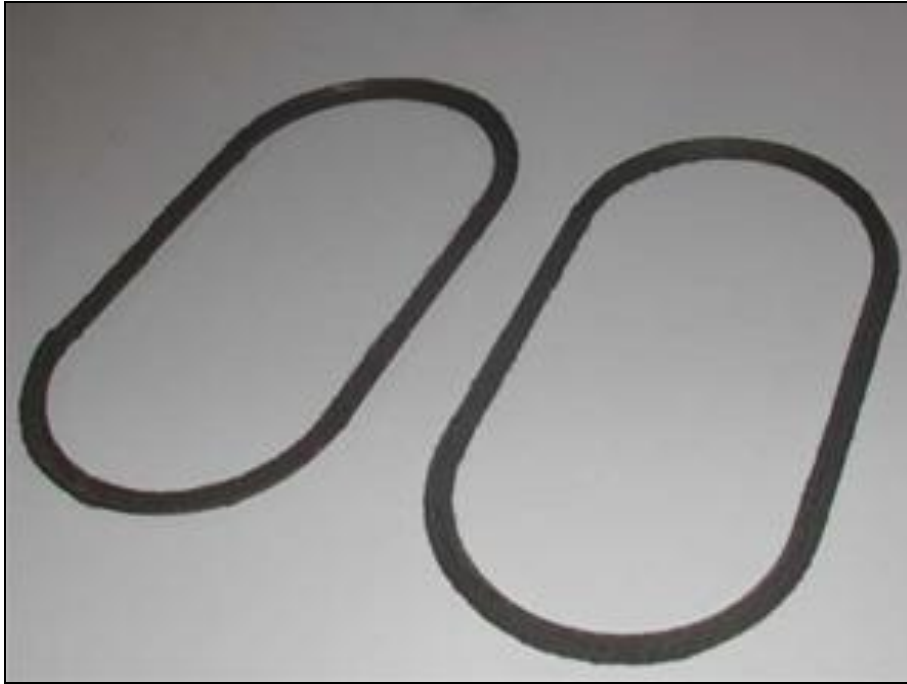


Figure 2.9 : V- Seal.

Axial seals are designed to provide axial support to the convertor mounting system. Axial seals are usually made of round wires to provide more gas permeation in the front surface of the seal. Figure 2.10 below shows a representative axial seal.



Figure 2.10 : Axial Seal.

2.4 Converter Can (Shell)

Converter can is exterior part of the catalytic converter. From the exterior to interior seals, mat mount, coated substrate are the parts that shell covers. Typical can known as the “Clam Shell” is made of 409 SS. Stainless steel shell thickness varies from 1, 2 to 2mm affected by the requirements of radiated heat and corrosion resistance. The

non-uniformity of the gas flow and excessive heat on the internal surface of the shell result in can deformation, noise and also bigger pressure drops.

2.5 Classification of the Catalytic Convertors from Location Point of View

Different types of catalytic convertors are used on the diesel and gasoline engines as the air fuel ratio and temperature range is totally different for these two types of engines. There are two main classification of the catalytic convertor from location point of view: close coupled catalytic convertor and underbody catalytic convertor.

2.5.1 Close-Coupled Catalytic Convertor

Close coupled catalyst is located $< 300\text{mm}$ after manifold pierce point or manifold/exhaust flange. Close coupled catalytic convertors take the advantage of the close location to the engine as the temperature of the exhaust gas is higher which is crucial for the chemical reaction activation. Placing the close coupled catalyst as close as possible to the exhaust manifold decreases light off time which is the time that activation of the chemical reactions take place [2]. The advancement in conversion efficiency is mainly influenced by the catalytic converter light-off characteristic as nearly 80% of emissions take place within the first three minutes of the cold start condition [6]. Location of the catalyst gives the ability of using the thermal energy of the exhaust gas before it reaches to the cold exhaust pipes resulting in decrease of gas temperature. However CCC performance from flow uniformity perspective is not satisfactory as pulsating exhaust gas flow cannot find enough space to fully expand before it goes through the monolith. Flow distribution and pressure drop are considered as two main design criteria of the CCC. Non uniform flow distribution causes hot spot in monolith, peak velocity locations and therefore results in poor conversion efficiency and undurable system that means either higher cost because of the excessive usage of the precious material or inability to succeed the emission legislations [4]. Inlet cone design has a major effect on the flow distribution of CCC, generally it is hard to design inlet cones since the packaging limitations. CCC are being used in most of the design as they give the opportunity of reducing the light off temperature and assisting to meet emission targets which is becoming more stringent day by day. A typical CCC design is given on Figure 2.11 below.



Figure 2.11 : Fiat 500 1.2 Lounge Close Coupled Catalytic.

2.5.2 Underfloor Catalytic Convertor

Underfloor catalytic convertor is located minimum 300mm far away from the manifold pierce point or manifold/exhaust flange before or after Y-Pipe. The main advantage of the underfloor catalytic convertor is the uniformity of the flow is pretty much higher than CCC as flow has enough space to fully expand. However exhaust gas temperature is comparatively lower as it is placed far away from the exhaust manifold resulting in the poor conversion efficiency and longer activation period. The ground clearance requirement of the catalytic convertor is another disadvantage as the underfloor convertor may need an additional protection to prevent any damage on the convertor caused by hillock, corner of the curb stone, etc [4]. Figure 2.12 below shows a representative underbody catalytic convertor.



Figure 2.12 : 2.0 TDCI Titanium Underfloor Catalyst.

2.6 Classification of Catalytic Convertors from Application Point of View

Two – Way Catalytic Convertor and Three- Way Catalytic Convertor are the main catalytic converter types used in automotive industry. Two – way catalytic converter is generally used on diesel engine application, three-way catalytic convertor is used on gasoline engine application.

2.6.1 Two-Way Catalytic Convertor

Two-way catalytic convertors which are also known as diesel oxidation catalyst (DOC) are used to convert carbon monoxide (CO) and hydrocarbons (HC) to carbon dioxide (CO₂) and water (H₂O) since 1990s. Another function of DOC is reducing the Particulate Matter (PM) by oxidizing the Soluble Organic Fraction (SOF). Although the capability of this reduction does not exceed 25–35%, emission level is sufficient for most of the engines developed with new technology comparing with the existing emission standard [1]. Two-way catalytic convertors do not have the ability to control the NO_x emissions. The basic chemical reactions taking place in the two-way catalytic convertor are:



This type of reaction needs higher oxygen ratio. Two way catalytic convertor technology can be applied to a wide range of diesel powertrain applications and used in European passenger and light duty vehicles also American heavy-duty diesel engines [1]. The restrictions on the usage of two way catalytic convertor are the engines which are produced before 1990s with an extremely high PM emissions, the engines with a very low operating temperature (below 200 C) and lastly the automotives using the diesel fuels that has higher than 500 ppm sulphur level [1]. Low sulphur fuel is preferred due to the propensity of the noble metals to convert SO_2 to particulate sulphates which deactivates the catalyst by restricting diffusion of the exhaust gases to and from the active catalyst sites.

Selection of precious metal type and ratio used on the DOC are determined due to the exhaust gases ingredient. The most common ones are Pt, Rh, Pd, Ni, CoO, PdO, CuO, Fe. These precious metals are held by highly porous alumina wash coat; the detailed section can be seen on the Figure 2.13. Al_2O_3 is the most common wash coat. TiO_2 and SiO_2 are also used in DOC application [4]. In order to prevent the oxidation of sulphur dioxide (SO_2) to SO_3 which can be resulted in the undesired sulphates and sulphuric acid formation, a silica wash coat is preferred over alumina, Pd is preferred over Pt [1].

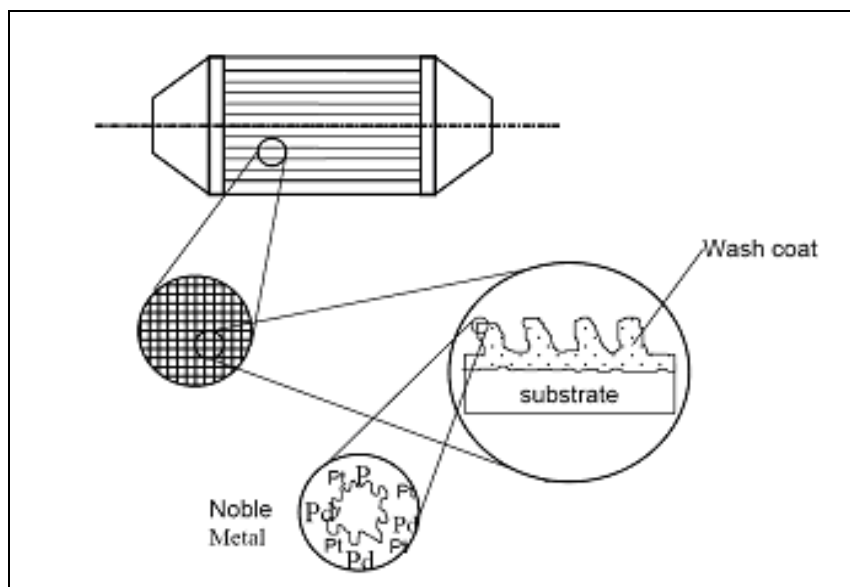


Figure 2.13 : Detailed Section of Alumina Washcoat.

As the emission regulations are becoming more stringent, DOC technology needs to be improved. Decreases in the light of time, HC conversion at the high temperatures are the most critical parameters in order to meet future emissions targets.

2.6.2 Three-Way Catalytic Convertor

Three-way catalytic convertors are being used in automotive industry in the beginning of 1980s. They are designed to convert the three pollutants: Carbon Monoxide (CO) to Carbon Dioxide (CO₂), Hydrocarbons (HC) to Water (H₂O), Oxides of Nitrogen (NO_x) to Nitrogen (N₂). Three-way catalytic convertors are also known as non-selective catalytic reduction, or NSCR. The main advantage of the TWC is the ability of controlling the NO_x emissions. In the reduction reaction, Rh is used as releasing factor for the oxygen atoms placed in NO_x. The oxygen atoms from the reduction reaction of NO_x are used to oxidise HC and CO.

The basic chemical reactions are given below:



The working conditions of catalytic convertor have crucial impact on the reaction efficiency. The Air/fuel ratio is the most common reference term used for mixtures in internal combustion engines. It affects the engine's operating characteristics. It is the ratio between the mass of air and the mass of fuel in the fuel-air mix at any given moment. The point at which air-fuel mixture is chemically balanced is known as stoichiometry (~14,7) where a complete burn can be achieved. The variation range of A/F ratio that catalytic converter works properly is operating window. In today's automotive technology oxygen (lambda) sensors are used to measure the oxygen concentration that helps to calculate the actual A/F ratio. Oxygen (lambda) sensors which are known as HEGO (Heated Exhaust Gas Oxygen), placed upstream of the convertor. The sensors placed downstream of the convertor known as CMS (Catalyst Monitor Sensor). These sensors give feedback to the Engine control unit. Control module uses the O₂ sensor's input to balance the fuel mixture, leaning the mixture when sensor reads rich, enriching the mixture when the sensor reads lean.

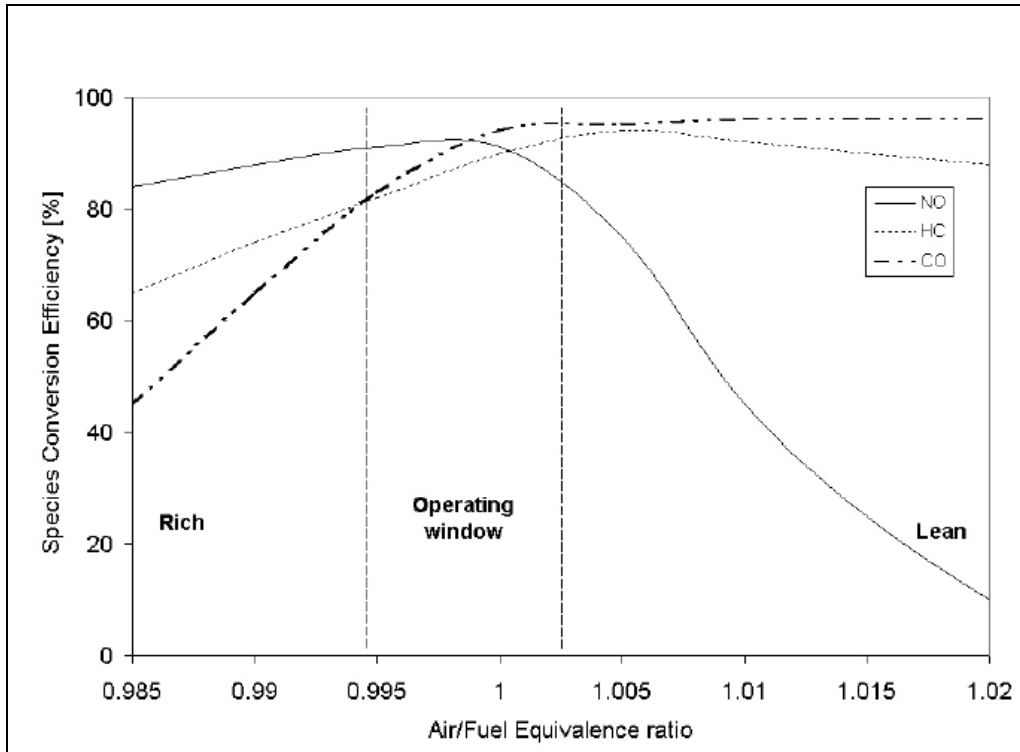


Figure 2.14 : A/F Ratio vs. Species Conversion Efficiency [1].

The definition of excess-air factor (λ) is:

$$\lambda = \frac{\text{quantity of intake air}}{\text{theoretical air requirement}} \quad (2.10)$$

A stoichiometric mixture has $\lambda = 1$, a lean mixture ($\lambda > 1$) contains more air; a rich mixture ($\lambda < 1$) contains less air. It is seen on the Figure 2.14 above the operating window condition gives the best efficiency rate combining HC, CO and NO_x emissions, if the air/fuel ratio is below stoichiometric, CO and HC emissions get higher due to the insufficient ratio of Oxygen. NO_x emission Conversion efficiency keeps going higher up to the stoichiometric value 1. If A/F ratio is above the stoichiometric that means the ratio of the oxygen is enough to oxidize CO and HC, the Conversion efficiency of these two gases is very high. On the other hand NO_x emission starts getting worse resulting in high emission. Conversion efficiency is very low for at least one pollutant outside of operating window conditions. [1] A typical TWC is showed on the Figure 2.15 below.

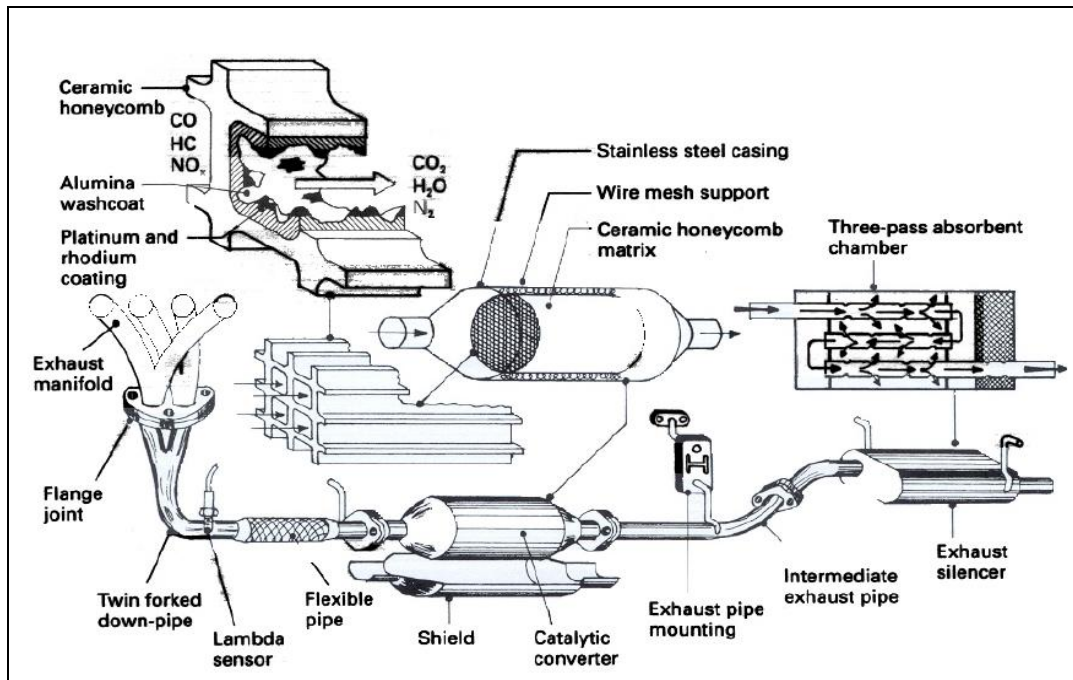


Figure 2.15 : Exhaust System with Underbody Catalytic Converter [1].

Three way catalytic converter does not activate before the temperature of converter inside reaches to a précised level (in the region of 550 K) which is called the light-off temperature. The most significant percentage of the harmful gases emitted to the nature in the period of cold engine start to fully warm up catalyst. The exhaust gases are not subjected to any chemical reaction as the temperature inside is not sufficient enough to activate the catalyst. The Figure 2.16 shows a study by Becker et al stated this ‘cold-start emission’ problem for Under Body Catalysts [7.]

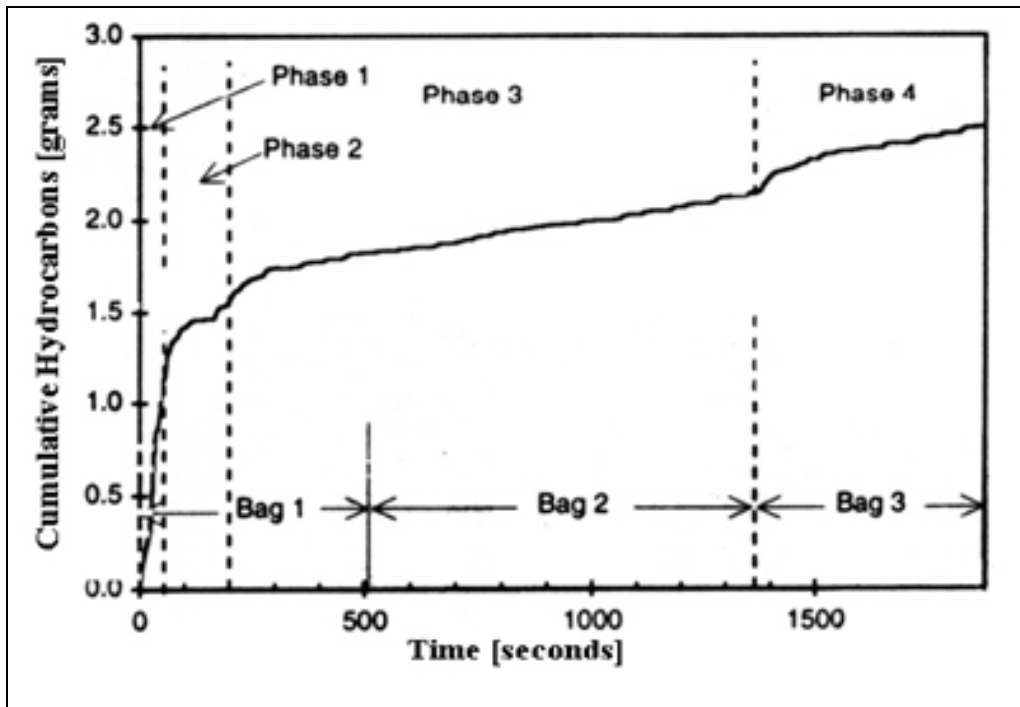


Figure 2.16 : Cumulative HC emission from cold start with an UNC [7].

The illustration shown on Figure 2.16 can also be equally applied to CO or NO_x emissions; there are four stages for a total cycle operation. First stage is the warm up stage in which fundamentally no chemical reaction takes place as the temperature is not sufficient enough for activation. Second stage is the light-off stage where there is a rapid increase in the catalytic reactions with increasing temperatures. Stage 3 is the stage where the reaction rates are fast enough and conversion is controlled with the mass transfer. Lastly stage 4 defined as warm start which is the restart after a ten minutes hot soak.

Cold start is a critical parameter to achieve the target as over 44% of the hydrocarbons are emitted during stage 1. In order to take the advantage of higher temperature just after the engine without heat losses in the connecting pipes Close Coupled Catalysts are used in most of the vehicle today. Generally Close Coupled Catalysts temperature inside is 100–200 C higher than Under-Body Catalysts.

2.7 Mathematical Modelling of Substrate

Engine performance is directly related with the exhaust backpressure value however, larger catalyst volumes are required in order to meet the emission target of the vehicle. As the emission standards becoming more stringent such as SULEV, it is needed to combine and calibrate vehicle, engine and the aftertreatment system

together as a power pack to achieve the targets of low emissions, fuel economy and engine performance. The pressure drop is sourced from the areas of exhaust system given below,

- Exhaust manifold
- Turbine and wastegate of the turbocharger
- Catalytic Converter(s)
- Piping
- Muffler
- Miscellaneous

Catalytic convertor substrate consists of many parallel channels that help the reaction conversion efficiency as the reaction area of the catalyst becomes larger. But it results in pressure drop due to friction loss as the exhaust gases pass through each channel. The channel diameter is around 1mm, which causes a laminar flow due to small Reynolds Number ($Re < 2300$). Therefore mathematical modelling of the pressure drop of the laminar flow in the channel can be made by using the Hagen-Poiseuille equation:

$$\Delta P = \frac{A \cdot \mu \cdot U \cdot L}{d_h^2} \quad (2.11)$$

A is the constant determined by the geometrical shape of the channel and d_h is the hydraulic diameter of the channel. Constant A is generally defined experimentally by measuring different types and shapes of the substrates. It can be found for most of the shapes in the literature.

Inlet and outlet flows before and after the substrate geometry also have effects on the overall pressure drop. Inlet effect on the pressure drop is based on the flow separation as exhaust gasses enter the channel with acceleration and bouncing to the walls of substrate. The outlet side pressure drops are due to the deceleration of the flow. The flow needs to take a distance for fully developed laminar flow. According to Langhaar this distance is; [8]

$$x = 0,0575 \cdot Re \cdot d_h \quad (2.12)$$

In the automotive applications Reynolds number for monolithic channels vary between 100-1000 therefore the required distance for fully developed laminar flow is 5 to 50 mm. The inlet and outlet effects for the pressure drop can be expressed as,

$$\Delta P = \frac{1}{2} \cdot \rho \cdot v^2 \quad (2.13)$$

which refers to kinetic energy of the incoming gas flow. The total pressure drop with respect to equation 2.12 and 2.13 is:

$$\Delta P = \frac{A \cdot \mu \cdot U \cdot L}{d^2_h} + \frac{B}{2} \cdot \rho \cdot v^2 \quad (2.14)$$

Here B needs to be determined. It is done by the residual analysis of the experimental data proposed by Fredrik Ekström and Bengt Andersson according to the equation below with different lengths, density, Reynolds number and OFA [8]. The results show that velocity has a quadratic dependence for the non laminar part of the equation 2.14 and other parameters have no explicit effect on the residual term according to Figure 2.17 [8]

$$\Delta P = \Delta P_{measured} - \frac{A \cdot \mu \cdot U \cdot L}{d^2_h} \quad (2.15)$$

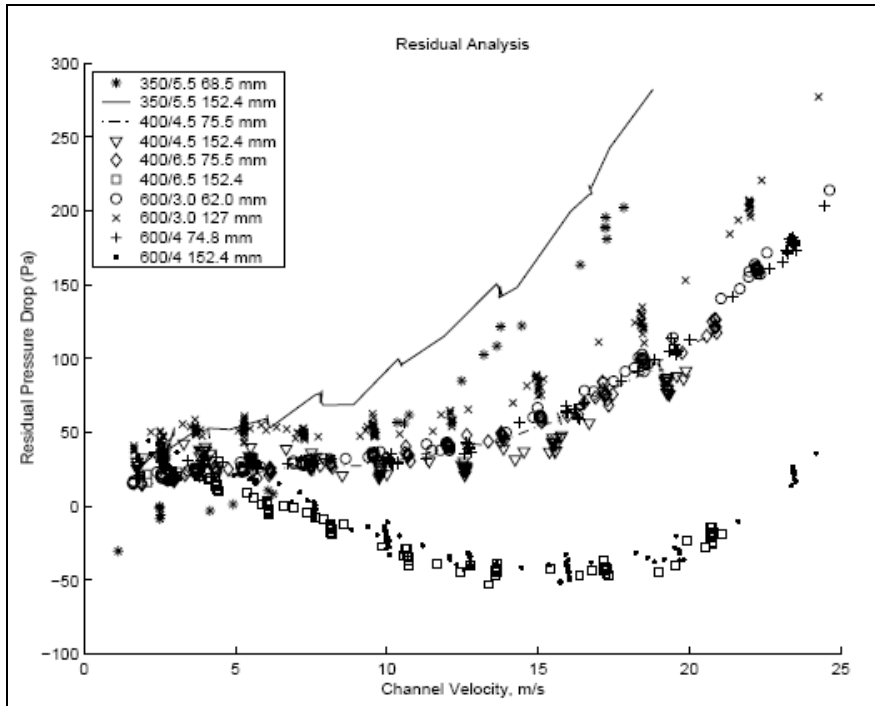


Figure 2.17 : Residual Pressure Drop according vs. channel velocity. [8]

B exhibits of a pure constant according to residual analysis. Regression gives the value $B = 0.41$ for the non-coated substrates. The model can be expressed as,

$$\Delta P = \frac{28.4 \cdot \mu \cdot v \cdot L}{d_h^2} + \frac{0.41}{2} \cdot \rho \cdot v^2 \quad (2.16)$$

The model shows a satisfactory consistence with the measured pressure drops for the uncoated substrates that can be seen on the Figure 2.18 below.

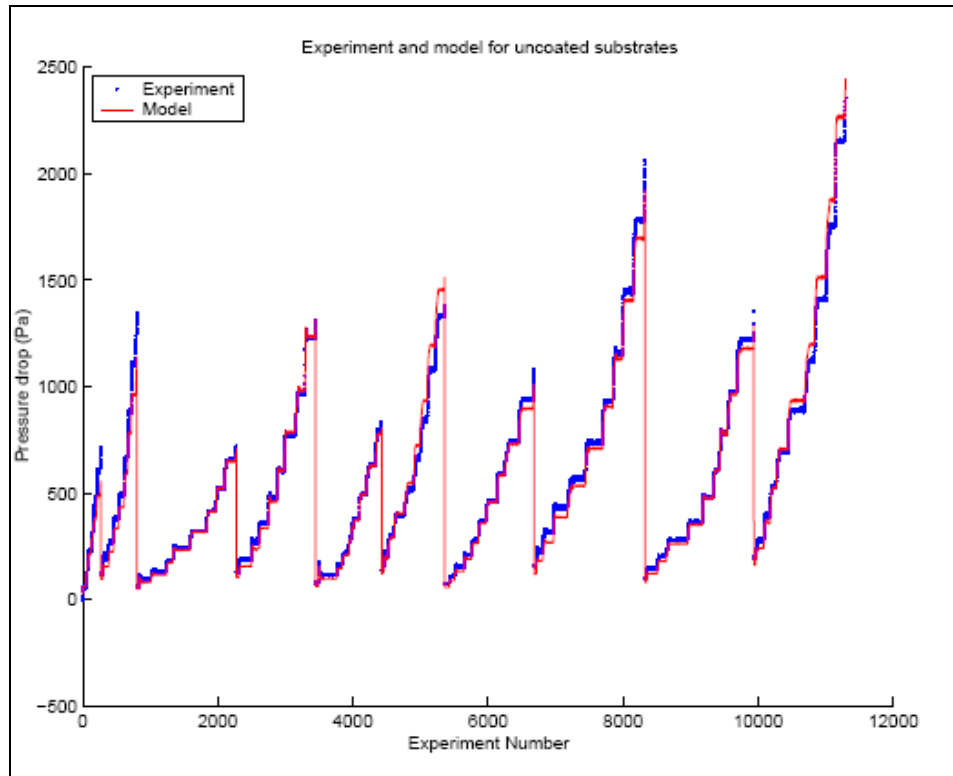


Figure 2.18 : Model and Experiment for Uncoated Substrates [8].

2.7.1 Catalyst Cell Shape Analysis

Fillet radius R , wall thickness and cell spacing L are the geometrical parameters that characterize the cell type as square, equilateral triangular, and equilateral hexagonal cell as shown Figure 2.19. [9]

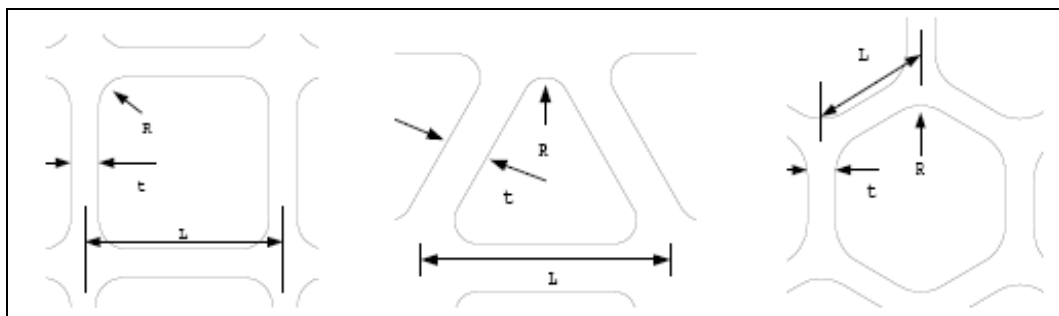


Figure 2.19 : Shapes of square, equilateral triangular and hexagonal cell [9].

The number of cells per square inch of cross-sectional area depicted as cell density of square cell:

$$N = 1/L^2 \text{ (cell/in}^2\text{)} \quad (2.17)$$

The wall area of square cell where wash coat is applied per unit volume is defined as geometric surface area:

$$GSA = \frac{4}{L^2} \left[(L-t) - (4-\Pi) \frac{R}{2} \right] \text{ (in}^2\text{/in}^3\text{)} \quad (2.18)$$

The ratio of open cell area to unit cross-sectional area is defined as open frontal area:

$$OFA = \frac{1}{L^2} \left[(L-t)^2 - (4-\Pi)R^2 \right] \text{ (dimensionless)} \quad (2.19)$$

The hydraulic diameter of square cell is defined below as

$$D_h = 4.OFA/GSA \text{ (in)} \quad (2.20)$$

2.8 Definition of Fundamental Parameters for Flow Uniformity Prediction

Computational Fluid Dynamics (CFD) has been widely used in the automotive industry to determine the gas flow distribution through the catalyst over the past decade. The main reason of this wide usage of steady/transient CFD simulations is its crucial role on the design of the after treatment system in contrast to time-consuming and costly experimental programmes. CFD does not replace the experimental measurements completely but the amount of experimentation can be reduced. The widely known commercial CFD software's are STAR-CD, FLUENT, FIDAP, etc. Two different 3-D CFD commercial codes are used in this thesis in order to compare the generated results' accuracy. The simulations were performed using the STAR-CD Version 3.26 and Fluent 6.3 solvers by applying a steady state compressible fluid flow simulation. The turbulence fields were calculated using the standard $k-\varepsilon$ turbulence model of Launder & Spalding, the near-wall region was handled using the standard 'wallfunction' approach. The basic parameters used in the catalytic convertor flow uniformity are explained in the following sub-sections.

2.8.1 Uniformity Index (Gamma Value)

Velocity distribution inside the catalytic convertor is very crucial as it causes an irregular use of area where reaction takes place and has effect on the catalyst durability. Uniformity index criterion is used in this study suggested by Welten to which integrates the velocity distribution profile over a section plane halfway between the front and back end of the substrate. Generally the uniformity index of the most systems today are above the 0,9 value, while the 0,88 is the acceptable criteria. 1.0 value refers to a totally uniform flow.

$$\gamma = 1 - \frac{\sum_{i=1}^n \sqrt{(U_i - \bar{U})^2} \cdot A_i}{2 \cdot \bar{U} \cdot A_{tot}} \quad (2.21)$$

where U_i is the gas flow velocity at cell 'i', \bar{U} is the mean gas flow velocity of the cross section, A_i is the flow area of cell 'i', A_{tot} is the total flow area of the cross-section, and 'i' is one of the 'n' cells in the cross-section [10].

2.8.2 Velocity Index

The velocity index is taken at a section plane halfway between the front end and back end of the substrate. Peak velocity location is in the normalized coordinate system. The X-axis (ranging from -1 to 1) defined as the major axis and the Y-axis (ranging from -1 to 1) defined as the minor axis. The distance from centre to peak velocity location combined with X, Y coordinates divided by the length of the line from centre to the edge of the monolith is defined as velocity index. This resultant is compared to a target value. (For a Velocity Index limit of 0,7 this would mean that if it is scaled the cross-section by 0,7 it would define the acceptable region for the location of the peak gas velocity.) [10]. The calculation method of the velocity index is explained below as:

$$\text{Velocity Index (VI)} = \frac{d}{R} \quad (2.22)$$

where R is the radius of the brick, d is the distance from centre of the plane in the brick to peak velocity location on the plane which is shown on the Figure 2.20 and calculated as follow:

$$d = \sqrt{((xl - x)^2 + (yl - y)^2 + (zl - z)^2)} \quad (2.23)$$

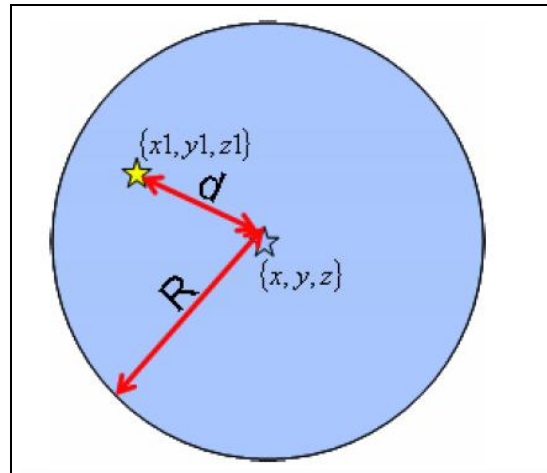


Figure 2.20 : Velocity Index.

2.8.3 Velocity Ratio

Ratio of the peak velocity to the area-weighted average velocity which is taken at a section plane halfway between the front end and back end of the substrate [10].

2.8.4 High Speed Area

The proportion of the cross sectional area of the monolith which has gas speed above 65% of the maximum velocity for the substrate which is taken at a section plane halfway between the front end and back end of the substrate [10].

2.8.5 Low Speed Area

The proportion of the cross-sectional area of substrate that has gas speed above 35% of the maximum velocity for the substrate taken at a section plane halfway between the front end and back end of the substrate [10].

2.8.6 Pressure Drop

Pressure difference (in psi or in kPa) across the selected planes. One plane is located upstream of the converter (e.g. cylinder head flange) and the other one is located downstream of the converter [10].

2.8.7 Porous Medium

Automotive catalytic convertor consists of several thousand small channels which will require huge computing resources to solve the flow details within every channel. In order to prevent this huge amount of work and time CFD uses an alternative

approach by assuming monolith as an equivalent continuum or porous medium with special properties [1].

The generalized porosity parameters are based on the pressure equations are expressed as:

$$\Delta P = \Delta P_{in-out} + \Delta P_{channel} \quad (2.24)$$

$$\Delta P_{in-out} = f \cdot \frac{(1.08 - 0.4OFA) + (1 - OFA)^2}{2d_h} + \rho \cdot v^2 \quad (2.25)$$

$$\Delta P_{channel} = \frac{K}{2d_h^2} \cdot L \cdot \mu \cdot v \quad (2.26)$$

In equations (2.25) and (2.26) OFA stands for the percentage of the open frontal area, d_h is the hydraulic diameter (m), v is the flow velocity in the channel, f is the correction factor to compensate the effects of coating thickness and K is the constant whose value depends on the cross-sectional shape of the channel, respectively. Generally K is taken 79 for square channel, 64 for round channel and 60 for sinuate channel [10].

The catalyst substrate is under debate as a porous medium on the 3D computational analysis programs, and the pressure drop equation across through the monolith is defined as,

$$\frac{\Delta P}{L} = -(\alpha V + \beta) \cdot V \quad (2.27)$$

in which V is the velocity over the whole section of the substrate and

$$\alpha = 0.5A \quad (2.28)$$

$$\beta = B\mu \quad (2.29)$$

where ρ and μ are the gas density and viscosity, respectively.

Velocity in equation (2.27) defined as velocity in the channel,

$$V = \frac{v}{OFA} \quad (2.30)$$

Then equation (2.25) can be defined as,

$$\frac{\Delta P}{L} = -\left(\frac{\rho}{2} \cdot A \cdot \frac{v^2}{OFA^2} + B \cdot \mu \cdot \frac{v}{OFA}\right) \quad (2.31)$$

The coefficients A and B are given below with respect to equation (2.28) and (2.29);

$$A = \frac{f}{L_h} \cdot \frac{(1.08 - 0.4OFA) + (1 - OFA)^2}{OFA^2} \quad (2.32)$$

$$B = \frac{K}{2d_h^2 OFA} \quad (2.33)$$

$$f = 0.73 + (1.05OFA^6) \quad (2.34)$$

A is known as the inertial resistance factor and B is known as the permeability [10].

2.8.8 Annular Velocity

Annular velocity is the proportion of the maximum annular velocity which is located just in front of the substrate along the rim of a layer of fluid cells to the average axial velocity on the same section. The annular velocity in each cell is defined in a local coordinate system based the topology of the individual cell where the substrate geometry is not circular as shown on the Figure 2.21 [10].

$$\text{Annular Velocity Ratio} = \frac{W_{\max}}{W} \quad (2.35)$$

where W_{\max} is the maximum angular velocity and W is average axial flow velocity.

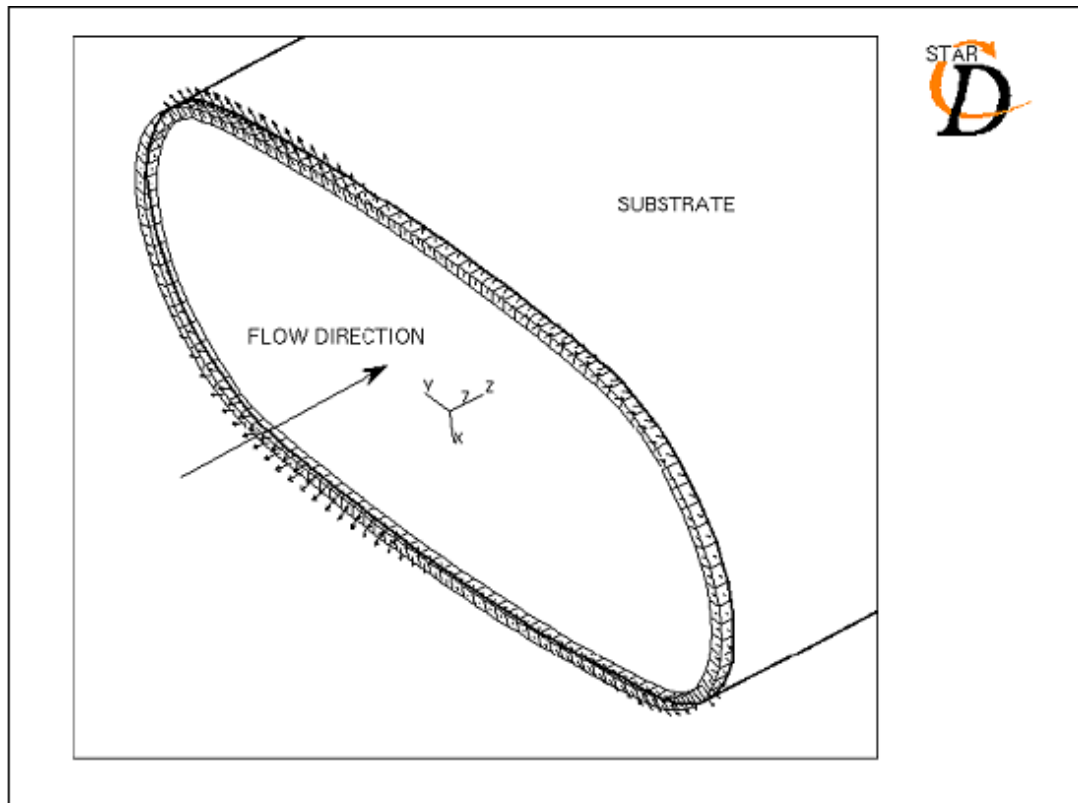


Figure 2.21 : Annular Velocity Plot of an Oval Substrate. [10]

2.9 Theoretical Models

STAR-CD is a code developed by Computational Dynamics Ltd. General purpose of this code is to simulate the three dimensional flow behaviour, pressure drop, heat transfer and other related areas based on Finite Volume (FV) method. [1] It involves a combination of pre-processor and post-processor PROSTAR and a main processor STAR. PROSTAR is the section where you import the geometry, the computational mesh, and determine the thermo physical properties of fluids/solids, turbulence models, solution parameters, and boundary locations. FV method is used to discretize the differential equations governing the conservation of mass, momentum, energy etc. within the fluid, and solved numerically by STAR.

Finally PROSTAR is used as the post processor taking the output data created by STAR.

General purpose of the FLUENT same as STAR-CD code is to predict the fluid flow, heat and mass transfer, chemical reaction and other related areas by solving the differential equations governing mathematical equations. Fluent analysis results are associated with redesigning of the products, product development, new designs and

troubleshooting. Fluent solvers are based on Finite Volume (FV) method. The fundamental steps of the CFD analysis as shown on the Figure 2.22 are:

- Problem definition and Processing
- Solver set up
- Post processing

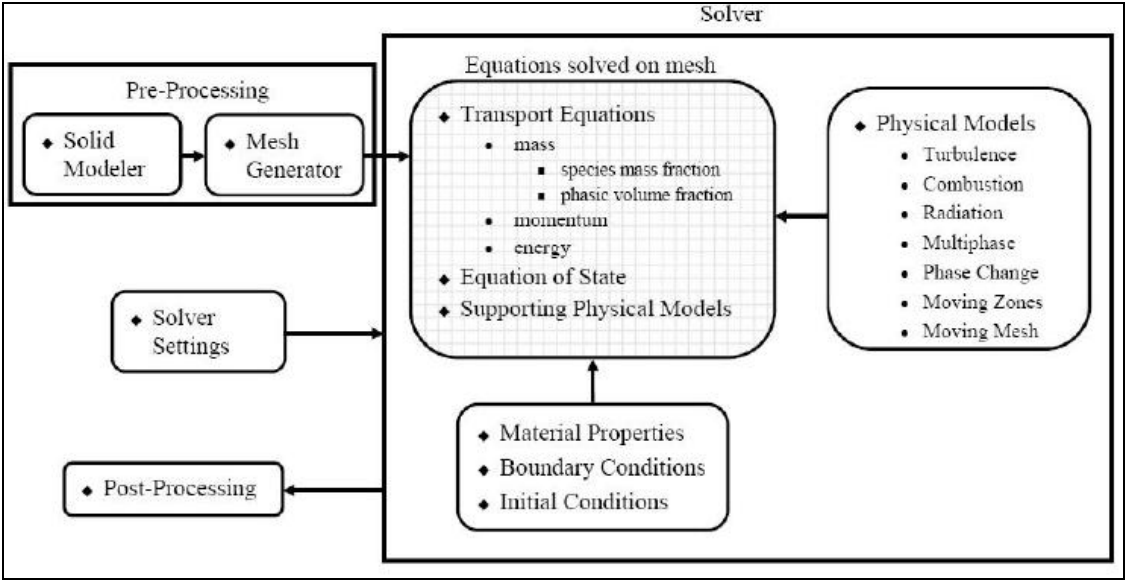


Figure 2.22 : CFD Process Overview.

2.9.1 Conservation of Mass

The mass of a closed system will remain constant, it cannot be created or destroyed. The continuity equation can be described by considering an arbitrary control volume as given on the Figure 2.23:

$$\frac{\partial \rho}{\partial t} + \frac{\partial(\rho u)}{\partial x} + \frac{\partial(\rho v)}{\partial y} + \frac{\partial(\rho w)}{\partial z} = 0 \tag{2.36}$$

In equation 2.36 ρ stands for density; t is time; x,y,z are the coordinates and u, v,w are the component of velocity along the x, y, z directions respectively [1].

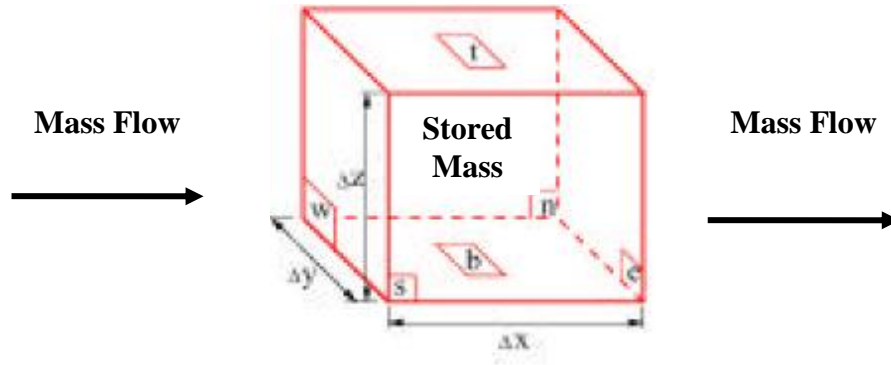


Figure 2.23 : Conservation of Mass.

The continuity equation written in vectored form for compressible flow is expressed below:

$$\frac{\partial \rho}{\partial t} + \nabla \cdot (\rho \vec{V}) = 0 \quad (2.37)$$

2.9.2 Balance of Momentum

The momentum principle is expressed as the rate of change in momentum is equal to sum of forces. [1] The Conservation of momentum defined as:

$$\frac{\partial}{\partial x_j} (\rho u_j u_i + \tau_{ij}) = -\frac{\partial p}{\partial x_i} + s_i \quad (2.38)$$

where s_i is the source term representing monolith resistance and the stress tensor (τ_{ij})

for Newtonian turbulent flow is:

$$\tau_{ij} = -\mu \left(s_{ij} + \frac{2}{3} \frac{\partial u_k}{\partial x_k} \delta_{ij} \right) + \overline{\rho u_i u_j} \quad (2.39)$$

in which δ_{ij} is the Kroneker delta and s_{ij} is the rate of strain tensor expressed as:

$$s_{ij} = \frac{\partial u_i}{\partial x_j} + \frac{\partial u_j}{\partial x_i} \quad (2.40)$$

2.9.3 Differencing Schemes

The discretization method is the process of the reduction of the continuum differential equations at a number of discrete locations. The general conservation equation is defined as:

$$\frac{d}{dt} \int_V \rho \phi dV + \sum_J \int_{S_j} (\rho \phi \vec{u}_r - \Gamma_\phi \text{grad} \phi) d\vec{S} = \int_V s_\phi dV \quad (2.41)$$

where ϕ is general dependent variable term, V is the random time-varying volume bordered by a moving closed surface S , V_p and S_j are the volume and discrete face of computational cell respectively, \vec{u}_r is the relative velocity between the fluid and the surface S , Γ_ϕ and s_ϕ are the general diffusion and source coefficients. First section on the left hand side of equation 2.38 is named as ‘transient term’, the second section on the left hand side is named as ‘flux term’ [1].

2.9.4 Turbulence Models

Turbulence models can be summarized in three categories as:

- Direct Numerical Simulation (DNS)
- Large Eddy Simulation (LES)
- Reynolds Averaged Navier Stokes (RANS) equations

The selection of the turbulence model for a given flow is generally based on the experience as the accuracy of the turbulence models depends on the nature of the flow. The standard k- ϵ model is used during the CFD analysis of catalytic convertor in order to determine the Reynolds stresses and turbulent scalar fluxes [1]. The standard k- ϵ model is a two equation eddy viscosity model which assumes that the turbulent Reynolds stresses and scalar fluxes on a time-averaged flow based expressed as:

$$\overline{\rho u_i u_j} = -\mu_t s_{ij} + \frac{2}{3} \left(\mu_t \frac{\partial u_k}{\partial x_k} + \rho k \right) \delta_{ij} \quad (2.42)$$

in which turbulent viscosity as a function of k and ϵ :

$$\mu_t = \frac{C_\mu \rho k^2}{\epsilon} \quad (2.43)$$

The turbulence energy k and the dissipation rate ϵ are derived from the transport equations given below:

$$\frac{\partial}{\partial x_j} \left(\rho u_j k - \frac{\mu_t}{\sigma_k} \frac{\partial k}{\partial x_j} \right) = \mu_t s_{ij} \frac{\partial u_i}{\partial x_j} - \rho \varepsilon - \frac{2}{3} \left(\mu_t \frac{\partial u_i}{\partial x_i} + \rho k \right) \frac{\partial u_i}{\partial x_i} \quad (2.44)$$

$$\frac{\partial}{\partial x_j} \left(\rho u_j \varepsilon - \frac{\mu_t}{\sigma_\varepsilon} \frac{\partial \varepsilon}{\partial x_j} \right) = C_{\varepsilon 1} \frac{\varepsilon}{k} \mu_t s_{ij} \frac{\partial u_i}{\partial x_j} - \frac{2}{3} \left(\mu_t \frac{\partial u_i}{\partial x_i} + \rho k \right) \frac{\partial u_i}{\partial x_i} - C_{\varepsilon 2} \rho \frac{\varepsilon^2}{k} + C_{\varepsilon 4} \rho \varepsilon \frac{\partial u_i}{\partial x_i} \quad (2.45)$$

where C_μ , σ_k , σ_ε , $C_{\varepsilon 1}$, $C_{\varepsilon 2}$, $C_{\varepsilon 3}$, $C_{\varepsilon 4}$ are empirical coefficients which are 0.09, 1.0, 1.22, 1.44, 1.92, 0.0, -0.33 respectively [1].

3. PROBLEM DEFINITION

The definition of the problem is designing a catalytic convertor that meets the ULEV emission target by using 3D CFD codes FLUENT and STAR-CD. Flow uniformity and velocity index targets which are set by the major manufacturers are taken as the acceptance criteria of the design.

3.1 Geometrical Constraints

The main constraint of designing a catalytic convertor is packaging. The exhaust system as a whole pack needs to be positioned and designed in a way that has the sufficient clearances to the surrounding components such as vehicle chassis, air conditioning system, and steering system. As the exhaust manifold is located just after the engine and close coupled catalysts are located as close as possible to the exhaust manifold there is not wide opportunity for packaging of the catalyst. Available catalytic convertor's volume needs to be maximized; on the other hand high concentrated and localized flows needs to be minimized for the chemical reaction efficiency. Uniform flow increases the useful life of the system, while reducing the risk of "in use" emissions and thermal, mechanical, chemical durability failures. As the most important parameter for the flow uniformity is inlet cone design which is indeed very difficult for the close coupled catalyst due to packaging constraints. Based on these constraints the geometry and the volume of the close coupled catalyst are selected and simulated.

The CFD analysis is applied to the close coupled catalytic convertor starting from exhaust manifold geometry. The length and diameter of the brick geometry respectively are 89mm and 118.4mm. The geometry details are shown on the Figure 3.1 below.

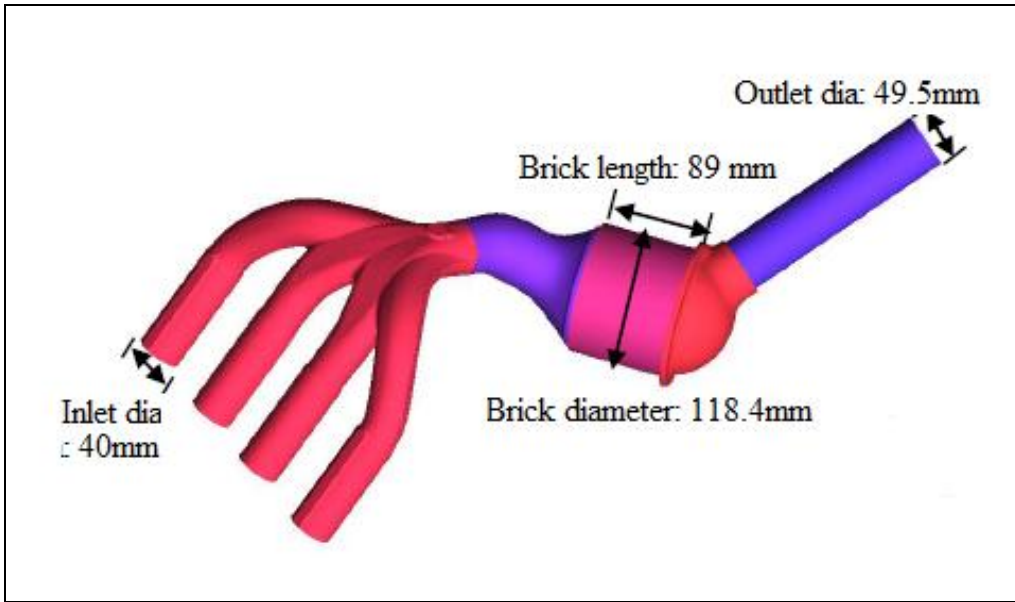


Figure 3.1 : Geometric Details of the CCC.

3.2 Physical Properties of Substrate

The cell structure of the generic substrate is usually expressed in cpsi/mil (cell per square inch/mill). 900/3 cpsi/mil square cell structure is used on this study. The unit of wall thickness is in mil and is a round number. The wall thickness is in mm. Since one mil is equal to 0,0254 mm, the actual wall thickness in mil will be: wall thickness (mm) / 0,0254. The wall thickness of 900/3 is 0.09 mm, so the actual wall thickness in mil will be $0.09/0.0254 = 3.54$. Details are shown on the Table 3.1. The effects of the coating thickness are not considered in this data and the correction factor f is applied to substrate with square channels.

Table 3.1: Physical Properties of Substrate

Generic Substrate (cpsi/mil)	Wall Thickness (mm)	Cell spacing (mm)	Bulk Density (g/cm ³)	Material Porosity (%)	Geometric Surface Area (cm ² /cm ³)	Hydraulic Diameter (mm)	Open Frontal Area (%)
900/3 (Square Cell)	0.09	0.84	0.28	26	42.3	0.76	80

3.3 Acceptance Flow Uniformity Criteria of the CCC

There are two major acceptance criteria that need to be checked to evaluate the design's acceptability. As explained on the previous section velocity index and the flow uniformity are the acceptance criteria that are set by the major automotive manufacturers. Details are given in the Table 3.2 below.

Table 3.2: CFD Acceptance Criteria of the Catalytic Converter

Criterion	Target Values
Flow Uniformity Index	Average of Runners ≥ 0.90
Velocity Index*	Average of Runners ≤ 0.70
*If flow uniformity index ≥ 0.94 , Velocity index is not required for acceptance	

Figure 3.2 which is shown below is an example of the CFD result plot of a catalytic converter flow simulation. Velocity index parameter in more detailed expressed as the peak velocity location of the substrate to be in the %70 area of the mid plane of substrate from the centre point to the edge of the substrate. Velocity index ≥ 0.7 is only acceptable when the flow uniformity index parameter is ≥ 0.94 . The reason for the velocity index target to be ≤ 0.70 is to protect the soot accumulation on the edge of the substrate that will cause Matt erosion and direct the exhaust gasses to localized flow. This will also end up as the loss and burnt of the support material accordingly movement and loss of substrate that is completely unacceptable from aftertreatment point of view.

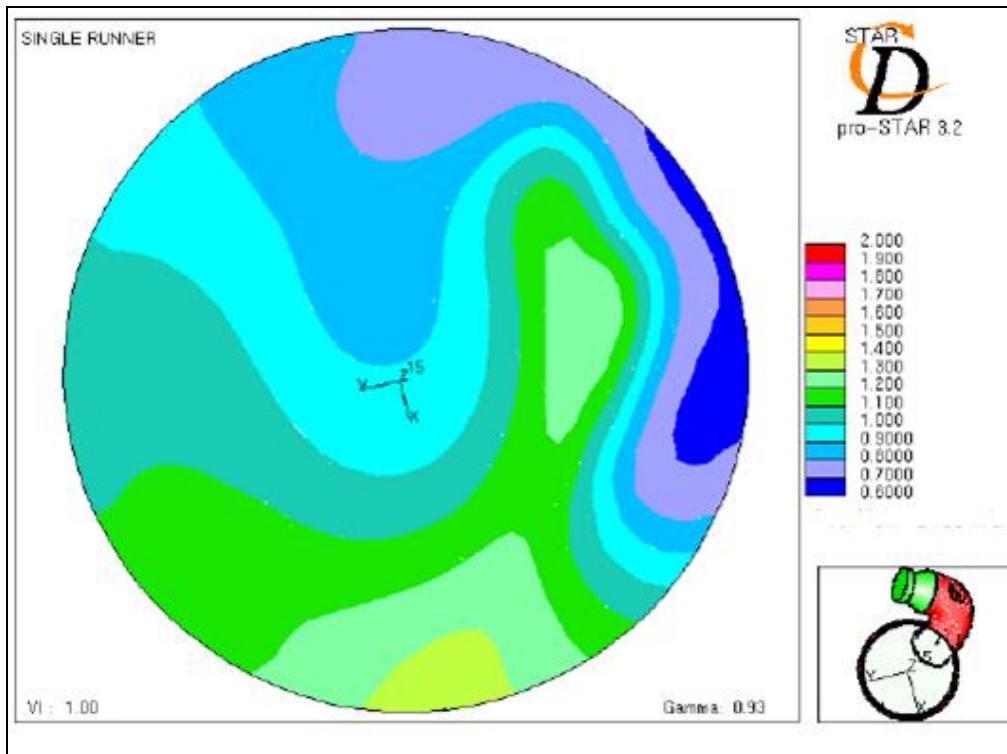


Figure 3.2 : Catalyst Gas Flow distribution Plot of the CCC. [15]

There are some other target values that are also taken to account by most of the manufacturers. These targets shown on the Table 3.3 below assist the reliability of the design but they should not be taken as a must.

Table 3.3 Target Values for Catalytic Converter CFD

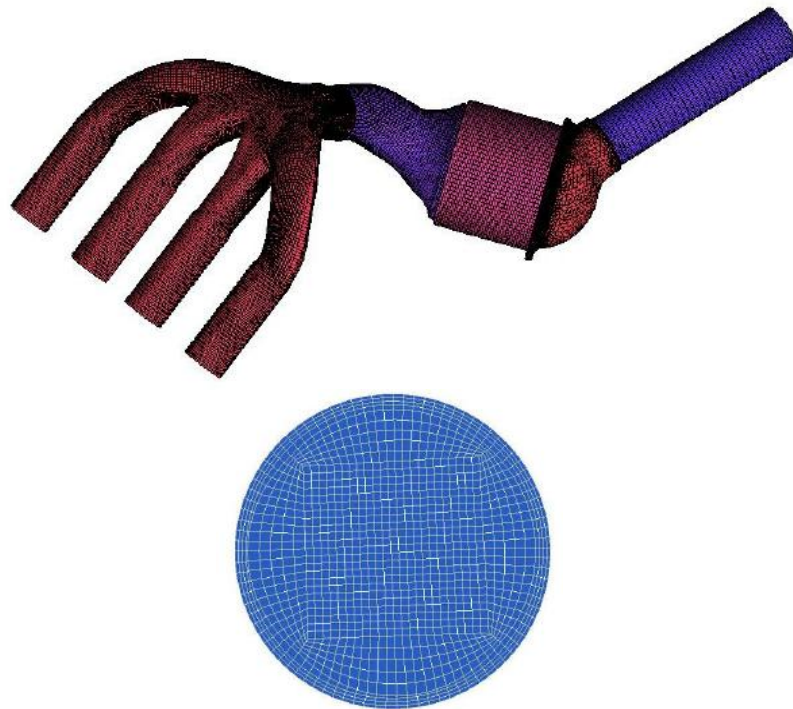
Criterion	Target Values
Velocity Ratio	≤ 1.70
High Speed Area	≥ 0.40
Low Speed Area	≥ 0.90
Annular Velocity	≤ 100

4. 3D CFD SIMULATIONS AND RESULTS

3D CFD simulations are performed using both the STAR-CD Version 3.26 solver and Fluent 6.3 solver in order to compare the results. The simulation and the results are given in details in this section.

4.1 Model Set-up and Mesh Structure Application of The Work

The computational mesh model of the exhaust system is created in ICEM-CFD. Mesh model is consisted of roughly 310,000 hexahedral cells which are shown in Figure 3.2. Arbitrary interface used between two hexahedral volumes and downstream with outlet cone is meshed with tetrahedral elements.



Mid plane of Brick

Figure 4.1: CFD mesh model used in the simulations.

Steady state compressible fluid flow was used for both analyses. The turbulence fields are calculated using the standard k-e turbulence model of Launder & Spalding, the near-wall region is handled using the standard ‘wallfunction’ approach. The

turbulence intensity and length scale at the inlet are 0.05 (5 %) & 0.004 m respectively. The fluid is assumed to be air at a specified temperature and absolute pressure. The initial temperature corresponds to the values specified at the inflow boundary. The compressible flow option selected so that density is calculated as a function of solved temperature and pressure, $\rho = \rho(P, T)$. The temperature equation is turned on. The analyses are performed with constant viscosity. The high Reynolds number standard k- ϵ turbulence model is used. All residuals are below 10^{-3} .

4.2 Boundary Conditions and Constraints

The inlet plane of the CFD domain was defined as an ‘inlet boundary’. The total mass flow rate is based on the cycle-averaged flow at peak power. The value is determined by an experimental measurement which is done by the calibration team of the manufacturer. The measurements are taken from engine dynamometer tests. The peak mass flow rate is defined as a value that is 1.4 times the measured cycle averaged mass flow. This is to encompass the effects due to the peak transient blow down pulse at full power. The temperature is based on the maximum temperature that is anticipated at the catalyst inlet (927°C). The fluid is assumed to be air at 927°C and absolute pressure. The boundary conditions used in the analysis are prescribed mass flow at the inflow region and pressure at the outlet.

The inlet boundary is taken as normal to the stream-wise direction of the flow which is achieved by creating a local coordinate system on the boundary. The turbulence intensity is assumed to be 5% and the length scale is 10% of the area-equivalent diameter of the inlet pipe.

The outflow region is defined as pressure type boundary.

The wall boundaries except the outer surface of the porous material region are specified as adiabatic, no-slip wall. Only outer surface of the porous material region is defined as a ‘slip’ wall (i.e. no shear flow) in order to retain the laminar flow throughout the substrate.

4.2.1 Porous Medium

The substrate in the catalytic converter is modelled as porous media and its flow characteristics are defined by the equations listed in Section 2. The equations

describe the pressure drop across an uncoated substrate at a specified cell density and wall thickness under the prescribed operation conditions. The flow path inside the channel is not modelled.

A local Cartesian coordinate system is used to specify the coefficients to model the substrate in the I (x), J (y) and K (z) directions. The flow is aligned with the K (z) direction. The Cartesian local coordinate system is defined at the front face of the substrate. Although its location is irrelevant to the subsequent calculation, this Cartesian local coordinate system is used for the post-processing and it is important that it is placed at the real centre of the substrate cross section. The recommended inertial resistance factor and permeability values in the I and J directions are 10^{-7} (Kg m^{-4}) and 10^{-7} ($\text{Kg s}^{-1} \text{m}^{-3}$), respectively. Figure 4.2 on the next page demonstrates how these values are defined via Prostar's Permeability and Porosity Factors panel. The analysis is conducted with one exhaust runner open and the others closed.

The summary of the boundary conditions are shown on the Table 4.1 below:

Table 4.1: Boundary Conditions

Boundary Conditions		
Domain	Type	Value
Inlet	Prescribed Mass Flow Rate	0.15867 kg/s
	CCC Inlet Gas Temperature	927° C
Outlet	Prescribed Pressure	10kPa
Catalytic Brick	Modelled as a porous medium, walls as slip boundaries	C2:= 10.81; C1:=8.55E+7
External Walls	No shear, Adiabatic	

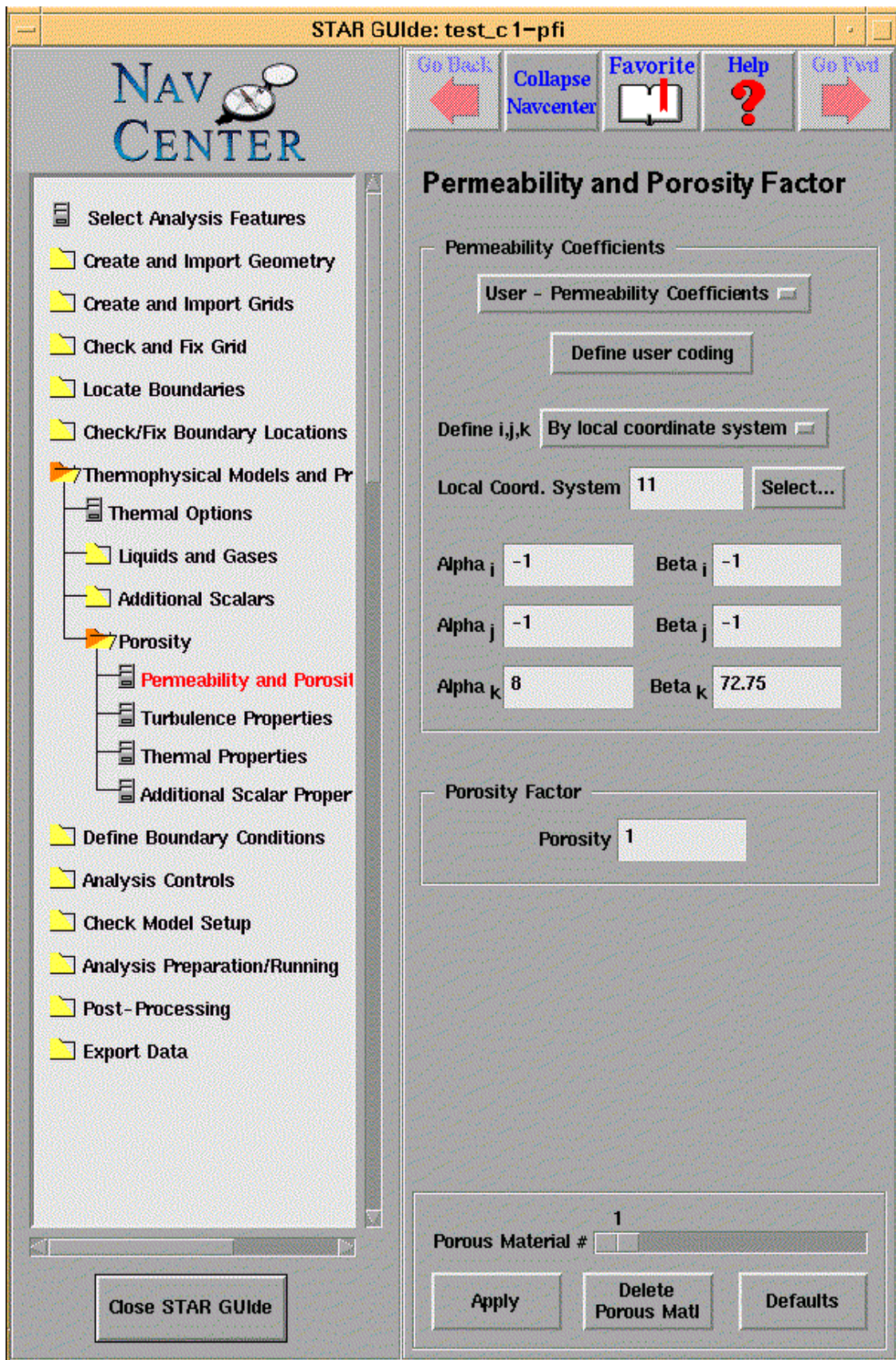


Figure 4.2: Simulation boundary set up plot for permeability and porosity factor.

4.3 Postprocessing

The analysis is simulated for each runner individually. The runner numbers are respectively shown on the Figure 4.3. The results of FLUENT and STAR-CD for each runner are shown relatively on the sub sections below.

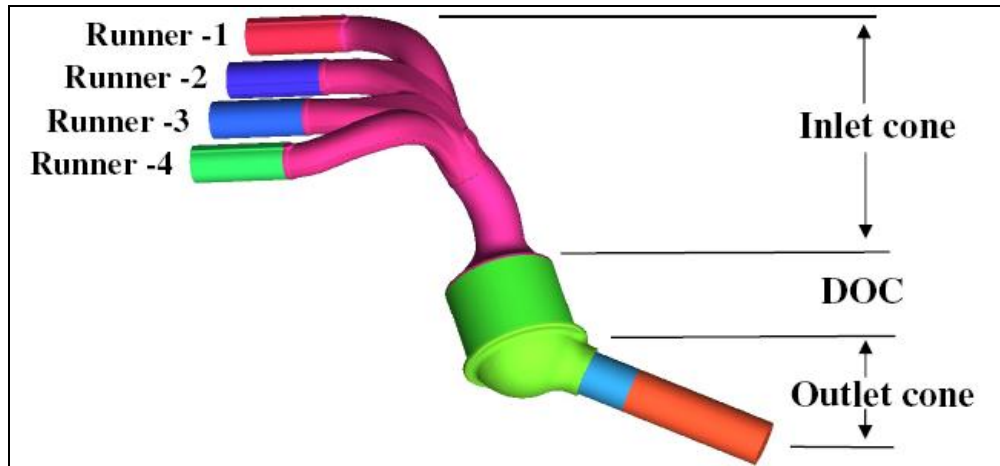


Figure 4.3: CCC Geometry Details.

4.3.1 First Runner Simulation Results

Gas flow distribution calculations are performed at a section plane halfway between the front end and back end of the substrate (DOC). Figure 4.4 and Figure 4.5 shows respectively STAR-CD and FLUENT code CFD plot of the first runner.

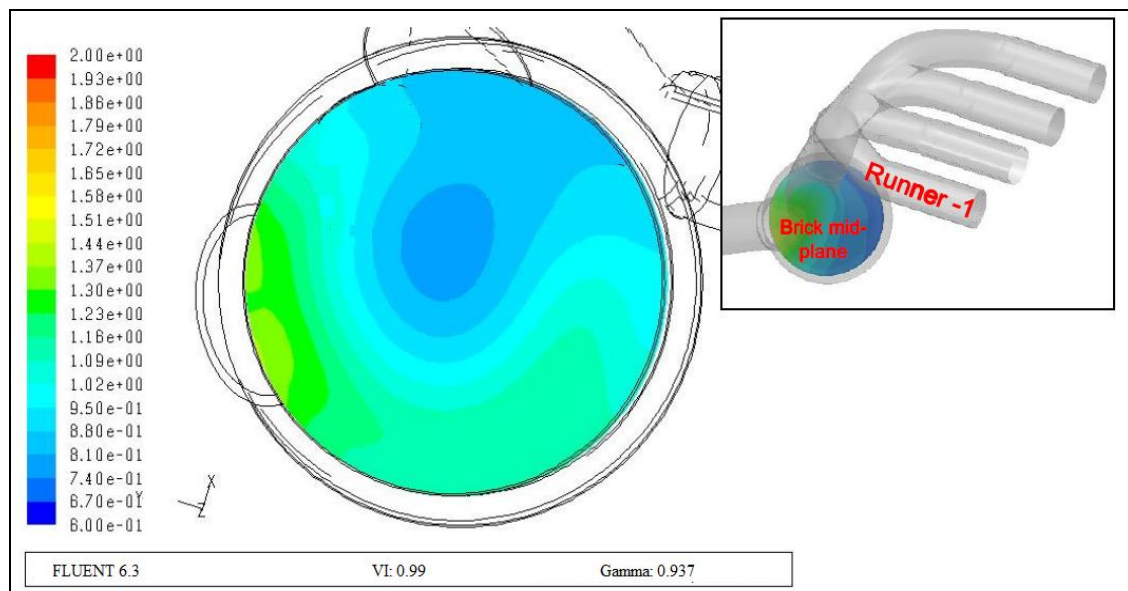


Figure 4.4: FLUENT Catalyst Gas Flow Distribution Plot of First Runner.

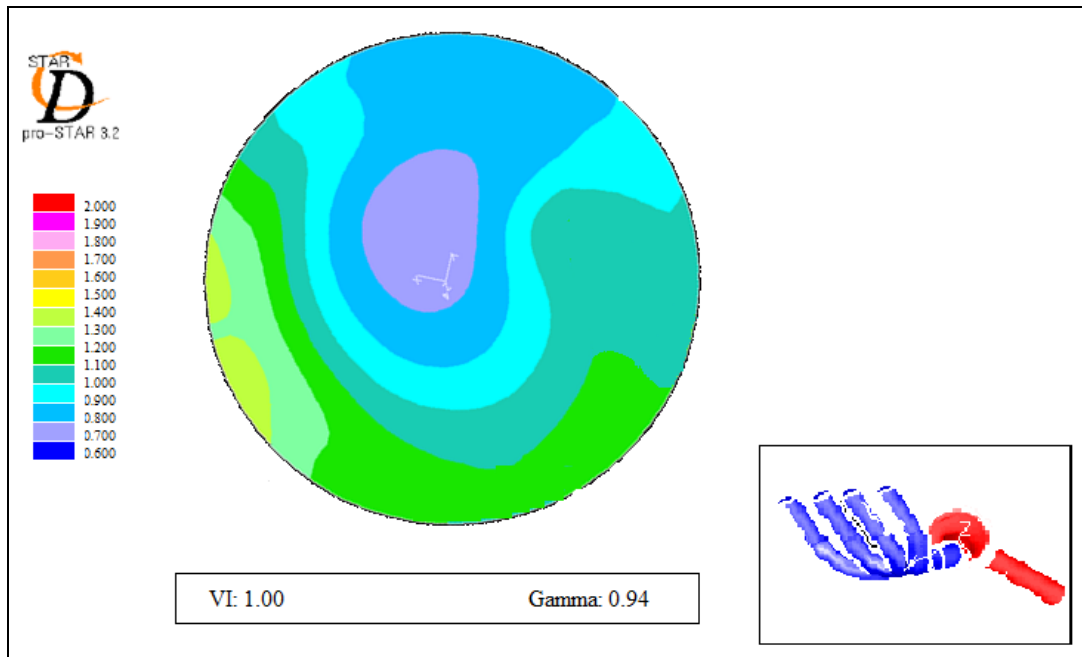


Figure 4.5: STAR-CD Catalyst Gas Flow Distribution Plot of First Runner.

Assessments of the first runner CFD results are:

- Velocity profiles of first runner shown on Figure 4.4 and Figure 4.5 are efficaciously close. The colour differences of the profiles are based on the different colour types and scales used on STAR-CD and FLUENT. The scale on the left hand side of the plot is the non-dimensional velocity which is divided by average velocity.
- VI result of first runner for the simulations respectively for FLUENT and STAR-CD are 0.9904, 1.0001. In normal conditions this VI value is unacceptable as it means the peak velocities are located on the edge of the substrate that may cause the support material loss but, this value can be acceptable as the Gamma value is equal to 0.94. Gamma value indicates that flow is highly uniform.
- Gamma Values are respectively 0.9370 for FLUENT, 0.9370 for STAR-CD that means design meets the requirements for Gamma as the values are above the limits described as recommended levels.
- The results of the STAR-CD and FLUENT analysis of first runner are given on the Table 4.2 below.

Table 4.2: Result Table of CFD Analysis of First Runner

	FLUENT ANALYSIS RESULTS	STAR-CD ANALYSIS RESULTS	TARGET
Uniformity index	93.70%	93.70%	≥ 90
Low Speed index	100	100	≥ 90
High Speed index	67.0411%	66.6313%	≥ 40
Velocity ratio= V_{max}/V_{avg}	1,3899	1,3943	≤ 1.70
Velocity index	0.9904	1.001	≤ 0.70

- The results for each analysis are correlated fairly well that prove the analysis's set up and run are correct.
- Total pressure drop value calculated from the inlet of the manifold to the outlet geometry of model is 44.62, 45.86 kPa for FLUENT and STAR-CD respectively.

4.3.2 Second Runner Simulation Results

Second runner simulation results are also taken from the section plane halfway between the front end and back end of the substrate. The velocity profiles plots taken from the FLUENT and STARCD codes are shown on the Figure 4.6 and 4.7 below.

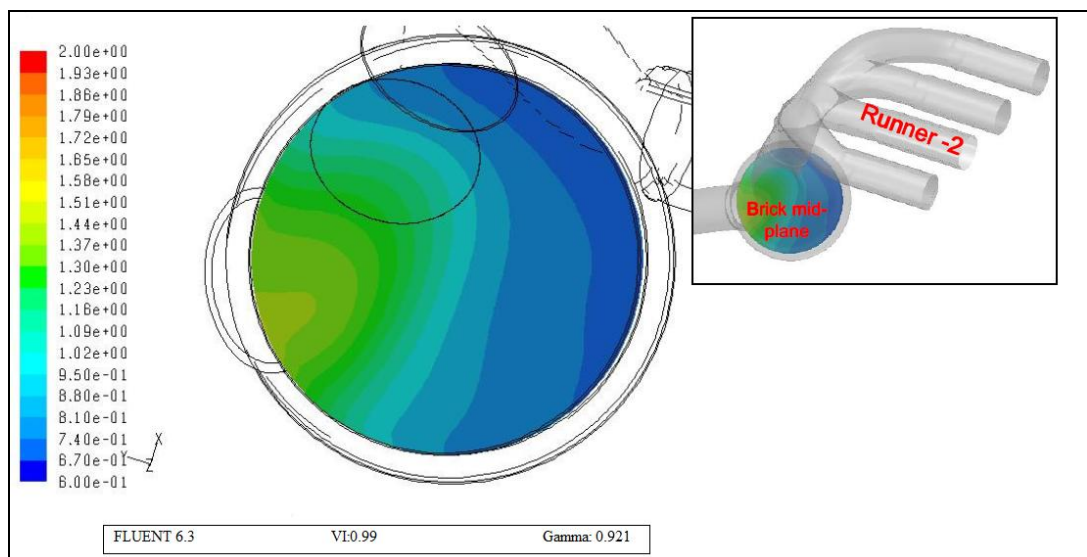


Figure 4.6: FLUENT Catalyst Gas Flow Distribution Plot of Second Runner.

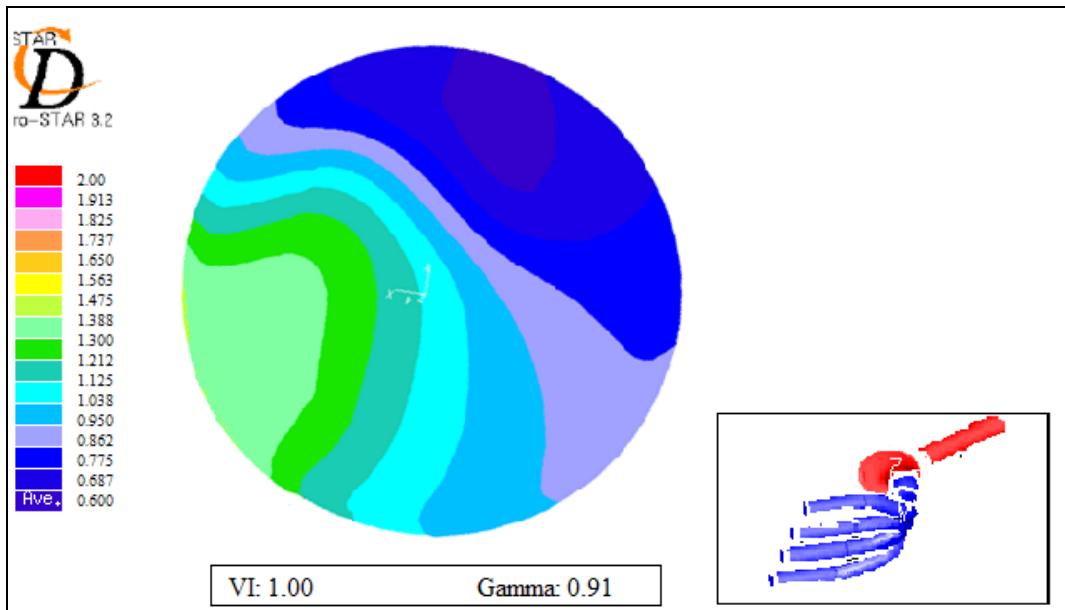


Figure 4.7: STAR-CD Catalyst Gas Flow Distribution Plot of Second Runner.

Assessments of the second runner CFD results are:

- Velocity profiles of the second runner have similar profiles which are shown on the Figure 4.6 and Figure 4.7. As stated on the first runner simulation results colour differences of the profiles are based on the different colour types and the scales used on STAR-CD and FLUENT.
- VI result of the second runner for the simulations respectively for FLUENT and STAR-CD are 0.99, 1.00. The velocity index value is close to meet the recommended value as the gamma values is close to 0.94 target.
- Gamma Values are respectively 0.916 for FLUENT, 0.918 for STAR-CD . The values are above the limits described as Recommended Levels meaning the flow is uniform enough but reduced compared to first runner.
- Second runner analysis total pressure drop value calculated from the inlet of the manifold to the outlet geometry of model is 36.29, 38.16 kPa for FLUENT and STAR-CD respectively.
- Table 4.3 shows the summary of the results for both Fluent and STAR-CD

Table 4.3: Result Table of CFD Analysis of Second Runner

	FLUENT ANALYSIS RESULTS	STAR-CD ANALYSIS RESULTS	TARGET
Uniformity index	91.60%	91.80%	≥ 90
Low Speed index	100	100	≥ 90
High Speed index	54.5947%	54.6169%	≥ 40
Velocity ratio= V_{max}/V_{avg}	1,4854	1,4673	≤ 1.70
Velocity index	0.9901	1.001	≤ 0.70

- It is shown on the Table 4.3 that the target values are achieved for the CFD analysis and FLUENT and STAR-CD analysis support each other as the results are well matched.

4.3.3 Third Runner Simulation Results

Third runner velocity profiles are shown on the Figure 4.8 and 4.9 for FLUENT and STAR-CD respectively

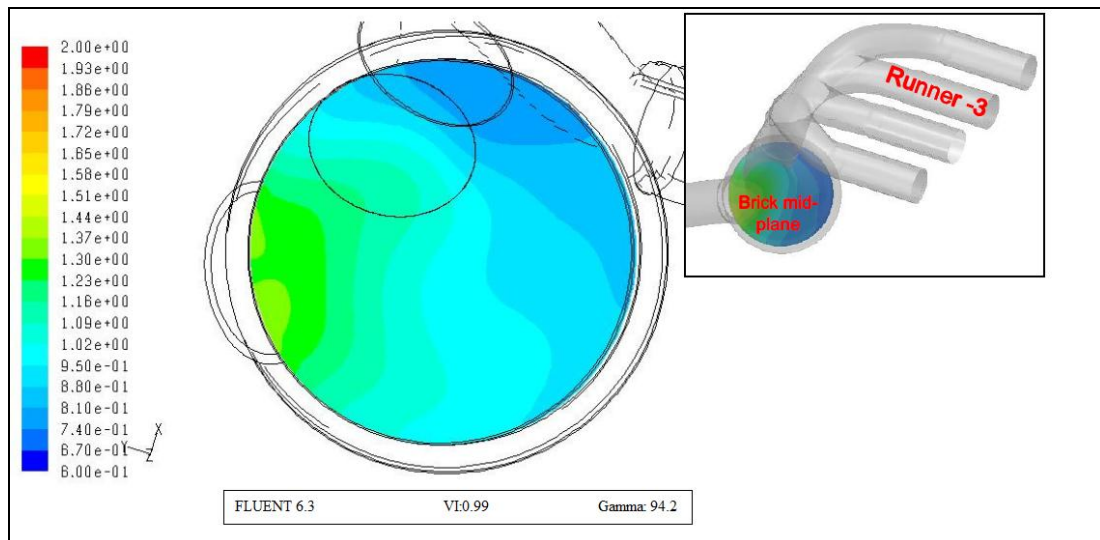


Figure 4.8: FLUENT Catalyst Gas Flow Distribution Plot of Third Runner.

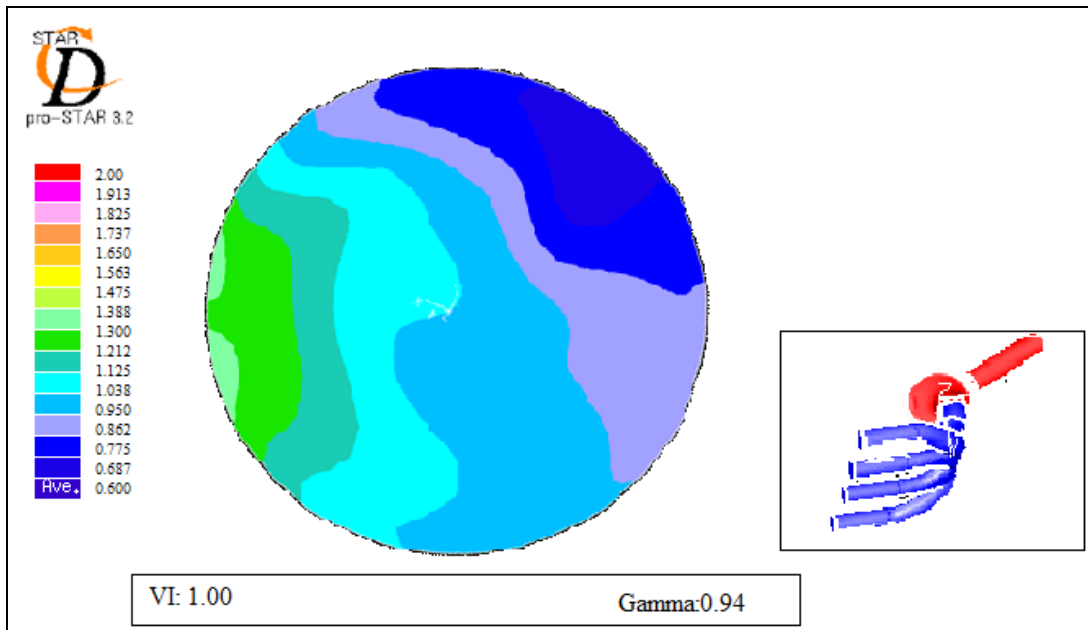


Figure 4.9: STAR-CD Catalyst Gas Flow Distribution Plot of Third Runner.

Assessments of the third runner CFD results are:

- Velocity profiles of the third runner has adequate similarity which can be seen on the Figure 4.6 and Figure 4.7. Colour differences of the analysis are based on STAR-CD and FLUENT different colour scale and type as mentioned on the first and second runner results.
- 0.99, 1.00 are the VI result of the third runner respectively for FLUENT and STAR-CD. It is not required to meet the velocity index target as the Gamma value is higher than 0.94.
- Gamma Values are respectively 0.942 for FLUENT, 0.949 for STAR-CD. The values are above the limits described as Recommended Levels. The flow is very close to be completely uniform.
- The summary of the results for both Fluent and STAR-CD are shown on the Table 4.4 below

Table 4.4: Result Table of CFD Analysis of Third Runner

	FLUENT ANALYSIS RESULTS	STAR-CD ANALYSIS RESULTS	TARGET
Uniformity index	94.21%	94.97%	≥ 90
Low Speed index	100	100	≥ 90
High Speed index	77.1380%	77.4350%	≥ 40
Velocity ratio= V_{max}/V_{avg}	1,3801	1,3742	≤ 1.70
Velocity index	0.99	1.001	≤ 0.70

- The result of the analysis for both FLUENT and STAR-CD are correlated sufficient enough as seen on the Table 4.4 above. The results are above the recommended level except velocity index but it is not required to meet the target as Gamma value is higher than 0.94.

4.3.4 Fourth Runner Simulation Results

Velocity profiles of the fourth runner are shown on the Figure 4.10 and Figure 4.11 respectively for FLUENT and STAR-CD.

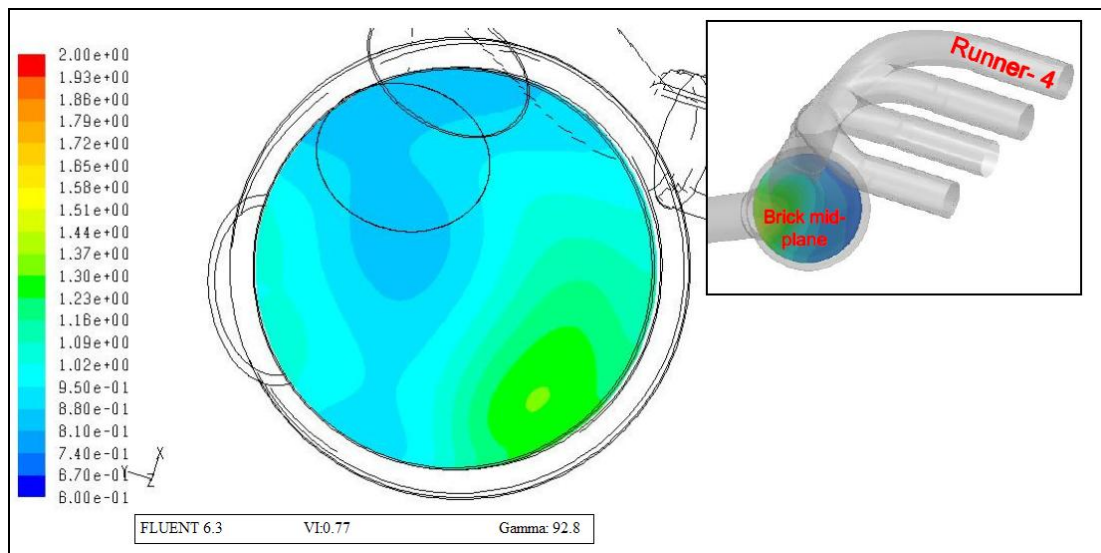


Figure 4.10: FLUENT Catalyst Gas Flow Distribution Plot of Fourth Runner.

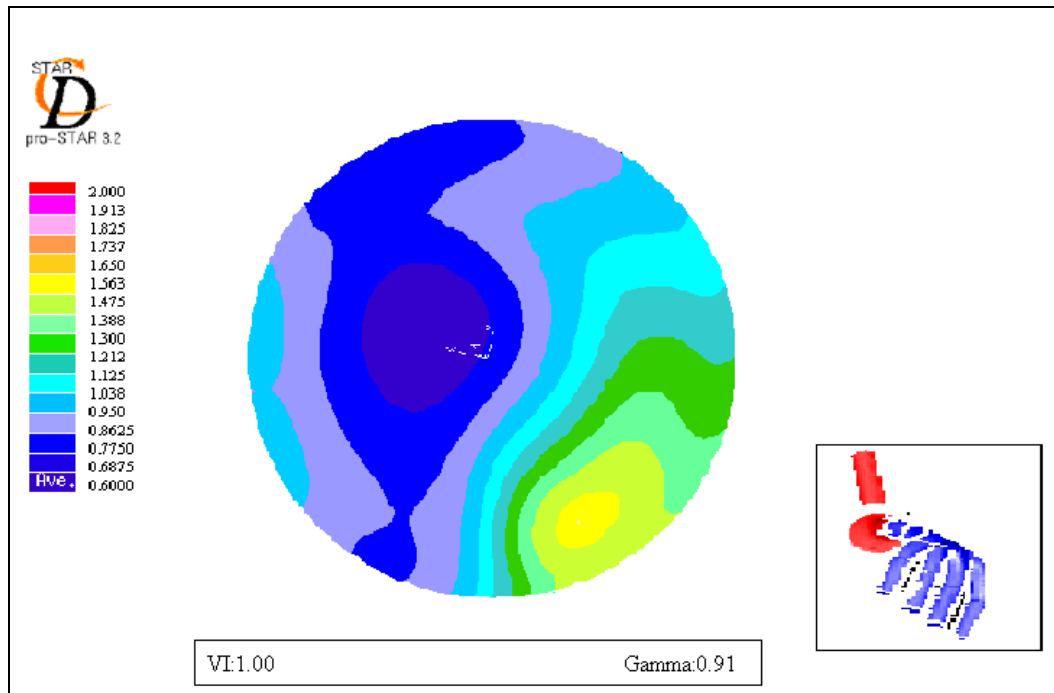


Figure 4.11: STAR-CD Catalyst Gas Flow Distribution Plot of Fourth Runner.

Assessments of the fourth runner CFD results are:

- A velocity profile of the fourth runner has adequate similarity which can be seen on the Figure 4.10 and Figure 4.11.
- VI value is 0.77 for both simulations FLUENT and STAR-CD. VI value is very close to meet the 0.7 recommended value and this is the best value compared to the other three runners.
- Gamma Values are respectively 0.9498 for FLUENT, 0.9497 for STAR-CD. Fourth runner Gamma value is the best compared to the other three runners which means the flow uniformity is very close to be completely uniform.

The summary of the results for both Fluent and STAR-CD are shown on the Table 4.5 below.

Table 4.5: Result Table of CFD Analysis of Fourth Runner

	FLUENT ANALYSIS RESULTS	STAR-CD ANALYSIS RESULTS	TARGET
Uniformity index	94.98%	94.97%	≥ 90
Low Speed index	100	100	≥ 90
High Speed index	40.3009%	40.3409%	≥ 40
Velocity ratio= Vmax/ Vavg	1,5014	1,5084	≤ 1.70
Velocity index	0.7752	0.7743	≤ 0.70

- The result shown on the Table 4.5 above for both FLUENT and STAR-CD are correlated fairly well and are above the target levels. VI value is off target but not required because of the Gamma value.

4.4 Engine Dynamometer Test

Engine dynamometer test which is also known as high speed dynamometer test is conducted in order to check the resistance of the catalytic convertor design to erosion, thermal shock and cracking. The test proved out that high VI values is not a risk for the brick internal durability. The test procedure can be explained briefly as follows:

- Engine runs till normal running temperature is reached. Then engine runs at Idle for 20 minutes.
- After Idle engine runs at maximum power speed for 160 minutes which is 3800 rpm.
- Running at Idle for 20 minutes than running at maximum power speed for 160 minutes refer to one cycle. The test is done with 60 cycles that took 180 hours in total.

High Speed Dynamometer test condition is quite severe in order to verify the total life time and severe situations based on either environment or driver.

The CCC is mounted to the engine dynamometer as shown on the Figure 4.12 below.

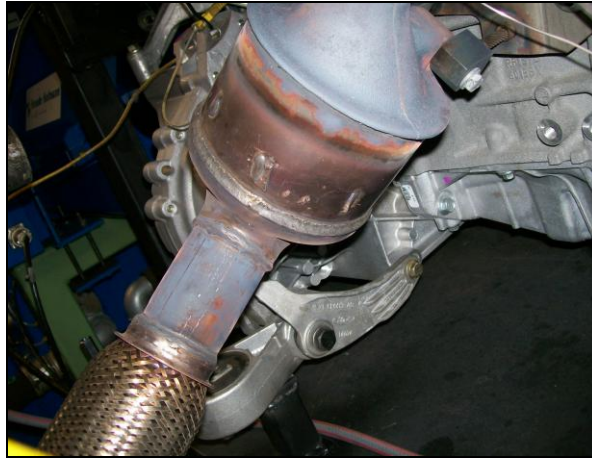


Figure 4.12: CCC Installation during HSD Test.

After 180 hour testing the parts are cut open. No any failure modes such as erosion, cracking or brick retention found on the CCC system. The brick inlet and outlet after the testing are shown on the Figure 4.13 on the next page.

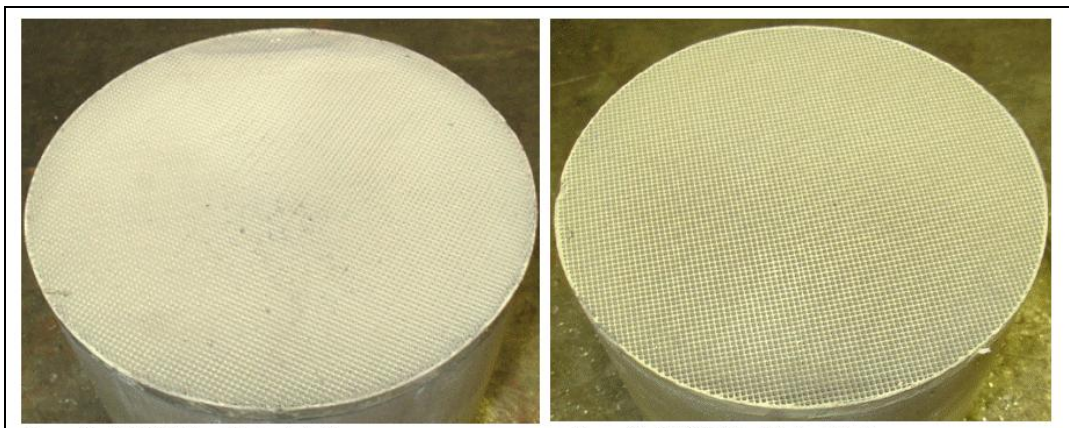


Figure 4.13: CCC Brick Inlet and Outlet after HSD test.

5. DISCUSSION AND CONCLUSION

It has been recognized in the automotive industry that the 3D steady state CFD analysis can provide us important information about how well the CCC system is designed and about where and what degree the flow through each exhaust pipe concentrates on the monolith. Although CCC suffers from the pulsating flow resulting in flow nonuniformity, it is known as an effective way in order to achieve the conversion efficiency. CCC inlet geometry is the most significant parameter of the catalyst design as it directly affects the flow distribution of the brick.

In this thesis, it has been demonstrated that the design of the CCC meets the requirements for Gamma. Values are above the limits described as recommended levels. The cases mentioned as Runner 3 and Runner 4 meet the requirements for the Velocity Index as well. The cases mentioned as Runner 1 and Runner 2 are close to meet the requirements for the Velocity Index. With the current geometry results of 93% flow uniformity, a good flow distribution is proved supporting emission conversion efficiency. There is also a good correlation between the FLUENT and STAR-CD analysis results regarding the velocity profile plots, flow uniformity, velocity index and all other attributes like velocity ratio, high speed area, etc... The engine dynamometer test can also be considered as a confirmation of CFD analysis as it proves the durability of the catalytic convertor design.

In conclusion, steady state CFD simulation is a very valuable tool to highlight performance as well as durability issues of the close-coupled design, where the inlet geometry has a crucial effect on gas flow uniformity, and possibly warrant a design change if necessary. Besides that using the CFD prediction method is a relatively efficient method compared to experimental methods considering time and cost.

REFERENCES

- [1] **Liu, Z.**, 2003: Pulsating Flow Maldistribution in Automotive Exhaust Catalysts - Numerical Modelling and Experimental Correlation, *PhD Thesis*, Coventry University, Coventry, UK.
- [2] **Cho, Y. J., Kim, Y. S., Han, M., Joo, Y., Lee, J. H., Min, K. D.**, 1998. Flow Distribution in a Close-Coupled Catalytic, *SAE Technical Paper Series*, no: 982552.
- [3] **Gulati, S. T.**, 1998: Comparing Physical Durability of Thin-Wall Ceramic Substrates, *SAE Technical Paper Series*, no: 982635.
- [4] **Duru, S.**, 2006: Optimization of a catalytic converter flow uniformity by CFD prediction, *M.Sc Thesis*, Istanbul Technical University, Istanbul, Turkey.
- [5] **Rajadurai, S., Jacob, S., Serrell, C., Morrin, R., Kircanski, Z.**, 2006: Durable Catalytic Converter Mounting with Protective and Support Seals, *SAE Technical Paper Series*, no: 2006-01-3419.
- [6] **Park, S., Cho, Y. J., Lee, S. Y., Kim, H. Y., Chung J. T., Yoon, K. J.**, 1999: Flow Analysis and Catalytic Characteristics for the Various Catalyst Cell Shapes, *SAE Technical Paper Series*, no: 1999-01-1541.
- [7] **Becker, E. R., Watson, R. J.**, 1998: Future Trends in Automotive Emission Control, *SAE Technical Paper Series*, no: 980413.
- [8] **Ekström, F., Andersson, B.**, 2002, Pressure Drop Of Monolithic Catalytic Converters Experiments and Modeling, *SAE Technical Paper Series*, no: 2002-01-1010.
- [9] **Park, S., Kim H. Y., Yoon, K. J., Cho, Y. J., Lee, S. Y.**, 1999: Flow Analysis and Catalytic Characteristics for the Various Catalyst Cell Shapes, *SAE Technical Paper Series*, no: 1999-01-1541.
- [10] **Leong, A.**, 2005. Steady State Analysis for Catalytic Converter Gas Flow Distribution, *Manufacturer Internal Document*, Dunton, England.

CURRICULUM VITAE

Candidate's full name : **Esra Gemici**

Place and date of birth : **Ankara 11/07/1983**

Permanent Address : **Girne Mah. Maden Sk. Kiptaş Blokları Daire:8
Maltepe/İSTANBUL**

**Universities and
Colleges attended** : **İTU / Mechanical Engineering**